Contents list available at CBIORE journal website

International Journal of Renewable Energy Development

Journal homepage: https://ijred.cbiore.id

Research Article

New alternative biodiesel (fatty acid butyl ester) production using microwave-assisted transesterification: kinetics and optimization

Indah Purnamasari[1], Suprapto Suprapto[2], Mahfud Mahfud[1]*

[1]*Department of Chemical Engineering, Institut Teknologi Sepuluh Nopember, Jl. Arief Rachman Hakim, Sukolilo, Surabaya 60111, Indonesia*

[2]*Department of Industrial Chemical Engineering, Institut Teknologi Sepuluh Nopember, Jl. Arief Rachman Hakim, Sukolilo, Surabaya 60111, Indonesia*

Abstract. Microwave-assisted transesterification represents a promising intensification strategy for rapid biodiesel processing. This study investigates the production of fatty acid butyl esters (FABE) from coconut oil via microwave-assisted butanolysis as an alternative to conventional methanol- or ethanol-based ester systems. Process optimization was performed using a face-centered central composite design (FCCD), with reaction time, temperature, and butanol-to-oil molar ratio as the principal variables. Under the optimized conditions, an approximately 98 % gravimetric product-recovery yield was obtained in less than three minutes. Kinetic analysis showed that the experimental data were better described by an apparent pseudo-second-order model under the investigated conditions; this model is interpreted as a lumped empirical description rather than proof of an elementary reaction mechanism. The evaluated fuel properties—density, kinematic viscosity, flash point, and cetane number—were within the corresponding limits specified by SNI 7182:2015 for those measured parameters only. Full SNI compliance and standardized quantitative total ester content were not established. Overall, the results demonstrate the feasibility of rapid microwave-assisted coconut-oil butanolysis while identifying important needs for improved feedstock characterization, quantitative ester analysis, replicated screening experiments, direct total-energy measurement, microwave-compatible temperature sensing, and solvent-recovery mass balancing.

Keywords: Microwave-assisted transesterification; Fatty acid butyl esters (FABE); Alternative biodiesel; Coconut oil; Butanolysis; Kinetic study; FCCD optimization; Renewable energy

@ The author(s). Published by CBIORE. This is an open access article under the CC BY-SA license (https://creativecommons.org/licenses/by-sa/4.0/).

Received: 14th January 2026; Revised: 17th August 2026; Accepted: 28th Sept 2026; Available online: 6th Oct 2026

1. Introduction

For over a century, global industrial development has depended heavily on fossil fuels—coal, petroleum, and natural gas—which still meet over 80 % of primary energy demand (Fernández-Tirado *et al.*, 2017; Harsono *et al.*, 2012). However, this reliance has come at a severe environmental cost. Fossil fuel combustion is a leading source of greenhouse gas (GHG) emissions, driving global warming (Gong & You, 2015; Hou *et al.*, 2011). Extraction processes further cause land degradation, water pollution, and ecosystem disruption, underscoring the urgent need for sustainable alternatives (Musharavati *et al.*, 2023).

In response, renewable fuels such as biodiesel have gained prominence. Biodiesel can be used in existing diesel engines with minimal modification, significantly lowering the carbon footprint compared to conventional diesel (Ashnani *et al.*, 2014; Font de Mora *et al.*, 2013). Indonesia, with its abundant agricultural resources, holds strong potential for biodiesel production from coconut oil—a feedstock with favorable properties for transesterification (Giraldi-Díaz *et al.*, 2018; Woo *et al.*, 2016). Coconut biodiesel offers benefits including reduced particulate emissions and improved public health outcomes (Maliyekkal & Shaija, 2021). Moreover, integrating renewable energy into biodiesel production can achieve a positive energy balance and lessen environmental impacts (Ashnani *et al.*, 2014; Chua *et al.*, 2010). Hence, while fossil fuels have historically enabled economic growth, their environmental toll necessitates a shift to renewables. Biodiesel derived from coconut oil in Indonesia presents a viable pathway to cut GHG emissions and advance sustainable energy. Continued technological development in this field is essential for a balanced and environmentally responsible energy future.

According to Badan Pusat Statistik (2024), coconut plantations in the country covered 3.33 million hectares in 2023, positioning Indonesia as a leading global coconut producer. Moreover, coconut exports reached 35.189 tons in 2024 (International Coconut Community, 2024). The abundance of this raw material provides a strategic advantage for the production of coconut-based biodiesel, offering opportunities to reduce reliance on fossil fuels while adding economic value to local agricultural resources.

Coconut oil is predominantly composed of triglyceride fatty acids, with approximately 91 % being saturated (Kaushik *et al.*, 2024). Lauric acid (48.7 %) is the major constituent, followed by myristic acid (18.9 %), caprylic acid (8.6 %), palmitic acid (7.6 %), and other fatty acids in smaller proportions (Seneviratne & Jayathilaka, 2016). Compared with common vegetable oils such as soybean or rapeseed oil, coconut oil contains a substantially higher proportion of medium-chain fatty acids (approximately

* Corresponding author
Email: mahfud@chem-eng.its.ac.id (M. Mahfud);

https://doi.org/10.61435/ijred.2026.62246
ISSN: 2252-4940/© 2026.The Author(s). Published by CBIORE

83 %). This compositional characteristic provides several advantages for biodiesel production, including improved oxidative stability, lower susceptibility to degradation, favorable cold-flow behavior, and higher cetane number, which collectively contribute to cleaner combustion and enhanced fuel performance.

Biodiesel is conventionally produced through an alcohol-catalyzed transesterification reaction, in which triglycerides are converted into fatty acid alkyl esters with glycerol generated as a by-product. Methanol is most commonly used as the alcohol reactant; however, its short carbon chain often results in biodiesel with inferior cold-flow properties. To address this limitation, higher alcohols such as butanol have attracted growing interest. The use of butanol produces butyl esters with longer alkyl chains, which improve fuel properties such as calorific value, cold-flow behavior, and oxidative stability. In addition, butanol can be produced renewably via biomass fermentation, further strengthening its sustainability profile. Owing to its greater hydrophobicity, butanol exhibits improved miscibility with oils and esters, resulting in a more homogeneous reaction system compared with methanol or ethanol (Sierra-Cantor & Guerrero-Fajardo, 2017; Hájek *et al.*, 2017). Alkaline catalysts, particularly sodium hydroxide (NaOH), are frequently employed due to their high catalytic activity, relatively low corrosiveness, and ability to deliver high biodiesel yields (Gaide *et al.*, 2023; Asaad *et al.*, 2023). Unlike methanol and ethanol, butanol exhibits higher miscibility with oils and esters, resulting in a more homogeneous reaction system. Butyl esters generally exhibit higher calorific values than methyl or ethyl esters because of their longer carbon chains (Nimcevic *et al.*, 2000). Notably, butanol forms a homogeneous phase with oils and esters, whereas methanol and ethanol typically generate biphasic systems. The longer carbon chain of butyl esters also contributes to higher heating values and lower cloud point temperatures, with previous studies reporting cloud point reductions of up to 10 °C compared with methyl esters derived from similar feedstocks (Sánchez *et al.*, 2015).

Traditional transesterification, however, relies on conventional heating methods that require high energy input, extended reaction times, and elevated pressures. These constraints not only hinder process efficiency but also increase costs, thereby limiting large-scale application. In response, microwave heating has been proposed as an innovative alternative to conventional heating. Microwave irradiation directly interacts with polar molecules through dipolar polarization and ionic conduction, generating rapid and uniform heating within the reaction medium. This mechanism significantly accelerates reaction kinetics, shortens reaction times, and simplifies product separation, making microwave-assisted transesterification a more energy-efficient and environmentally favorable approach (Gude *et al.,* 2013; Khan *et al.*, 2021).

Several studies have validated the advantages of microwave-assisted transesterification in biodiesel synthesis. (Nomanbhay & Ong, 2017) demonstrated that microwave heating improved reaction efficiency and reduced by-product formation. Similarly, Kurniati *et al.* (2019) reported substantial improvements in yield and ease of separation compared with conventional methods. Rachmaditasari *et al.*, (2024) further highlighted the potential of coconut oil, achieving a biodiesel yield of 99.89 % under optimized microwave power (443.9 W) and catalyst concentration (0.2 wt.% NaOH). Comparable findings by Mahfud *et al.* (2018), Cancela *et al.* (2012), and Maheswaran & Uthranarayan (2022) confirm the broad applicability of microwave technology in biodiesel synthesis.

Beyond improvements in yield and reaction rate, microwave-assisted transesterification offers notable flexibility toward diverse lipid feedstocks, including low-quality and waste-derived oils (Handayani *et al.*, 2018, 2019). This adaptability is particularly relevant for Indonesia, where feedstock availability may vary spatially and seasonally. Nevertheless, biodiesel production under microwave irradiation remains highly sensitive to operating parameters such as reaction time, temperature, catalyst concentration, and alcohol-to-oil ratio. These variables must be carefully optimized to maximize ester yield while minimizing undesirable side reactions, including saponification and emulsion formation (Garusti *et al.*, 2020). Moreover, most existing microwave-assisted studies focus predominantly on conventional fatty acid methyl or ethyl esters, leaving alternative ester routes insufficiently explored, especially in terms of kinetic behavior and systematic optimization. To the best of our knowledge, studies on microwave-assisted butanolysis of coconut oil for FABE production remain limited, particularly for medium-chain triglyceride feedstocks. Previous studies from our group focused on methyl ester and isopropyl ester systems, whereas the present study specifically investigates butyl ester synthesis, kinetic behavior, and process intensification under microwave irradiation.

Accordingly, this work proposes an integrated framework that combines microwave-assisted process intensification, kinetic modeling, and Face-Centered Central Composite Design (FCCD) optimization for FABE production from coconut oil. While microwave-assisted transesterification has been widely reported, its application to coconut oil butanolysis remains scarcely explored, particularly regarding reaction kinetics and multivariable optimization. The study demonstrates that microwave-assisted butanolysis can deliver ultra-rapid conversion (≤3 min) with high ester yield, highlighting the capability of microwave heating to mitigate kinetic and mass-transfer constraints often associated with longer-chain alcohols. By explicitly coupling kinetic analysis with FCCD-based optimization, the present work moves beyond empirical yield maximization and establishes an engineering-relevant operating window linking reaction behavior, controllable parameters, and biodiesel performance.

Therefore, this study aims to develop and evaluate a microwave-assisted transesterification route for producing FABE from coconut oil using NaOH as a catalyst. Specifically, it seeks to: (i) assess the feasibility of coconut oil butanolysis under microwave irradiation, (ii) elucidate the reaction kinetics under intensified heating, and (iii) optimize key operating variables (reaction time, temperature, and alcohol-to-oil molar ratio) using FCCD to maximize yield while maintaining process practicality. The resulting framework provides quantitative guidance for process intensification and offers a transferable methodology for designing energy-efficient and flexible biodiesel systems based on locally available renewable feedstocks, with outputs that support subsequent scale-up considerations through an engineering-oriented process map connecting operating conditions to conversion performance and product quality.

2. Material and Method

2.1 Material

In this experiment, the raw material used was Barco Co. coconut oil, sourced from a local supermarket. Before transesterification, the coconut oil feedstock was characterized by free fatty acid (FFA) content, acid value, and moisture content. The analysis

showed that the coconut oil contained 0.245 wt% FFA, had an acid value of 0.69 mg KOH g^{-1} oil, and a moisture content of 0.061 wt%. These relatively low values indicate that the feedstock was suitable for alkali-catalyzed transesterification and minimized the possibility of soap formation, catalyst consumption, and hydrolysis reactions during biodiesel production. The butanol (99 % purity) used as the alcohol reactant was procured from CV. Chemindo Multi Sentosa, Surabaya, which also supplied the sodium hydroxide (NaOH, 99 % purity) catalyst.

2.2. Determination of Free Fatty Acid, Acid Value, and Moisture Content Of Coconut Oil

The free fatty acid (FFA) content of the coconut oil was determined by acid-base titration. A 5 mL oil sample, with known density at room temperature, was placed in a 250 mL Erlenmeyer flask and dissolved in 50 mL of 95 % ethanol. Subsequently, 1 mL of phenolphthalein indicator was added, and the mixture was titrated with standardized NaOH solution until a stable pale pink endpoint was maintained for 15 s. The volume of NaOH consumed was recorded and used to determine the acid value and FFA content. All analyses were conducted in triplicate.

$$\text{FFA (\%)} = \frac{\text{V NaOHx N NaOH x } M_{\text{w fatty acid}} \text{ x 100 \%}}{W_{\text{sample}} \text{ x 1000}}$$

The acid value of coconut oil was determined by an acid–base titration method. Approximately 2–5 g of the oil sample was accurately weighed into a 250 mL Erlenmeyer flask and dissolved in 50 mL of a neutralized ethanol–diethyl ether mixture (1:1, v/v). Subsequently, 2–3 drops of phenolphthalein indicator were added. The solution was titrated with 0.1 N ethanolic KOH under continuous stirring until a faint pink color persisted. All measurements were conducted in triplicate.

$$\text{Acid Value } \left(\frac{\text{mg KOH}}{\text{g}}\right) = \frac{\text{V x N x 56.1}}{\text{m}}$$

where V is the volume of KOH used for sample titration (mL), N is the normality of the KOH solution, m is the mass of the oil sample (g), and 56.1 is the molecular weight of KOH (g mol^{-1}).

The moisture content of the coconut oil was determined using a gravimetric drying method. Approximately 5 g of coconut oil was weighed into a pre-dried and pre-weighed container. The sample was heated in an oven at 105 °C for 20 min, cooled to room temperature in a desiccator, and reweighed. The heating, cooling, and weighing procedures were repeated at 20 min intervals until a constant weight was achieved. The moisture content was calculated from the weight loss during drying according to this Equation :

$$\text{Moisture Content (\%)} = \frac{W_i - W_f}{W_i} \text{ x 100 \%}$$

where W_i is the initial sample weight (g) and W_f is the final weight after drying (g).

2.3 Apparatus and Methods

A biodiesel reactor unit (Fig. 1) uses a 1000 mL two-neck Pyrex flask connected to a microwave. The microwave used is an Electrolux model EMM-2308X, with the following specifications: Voltage: 220 V / 1250 W, Maximum power: 800 W, Maximum time: 35 minutes, Magnetron frequency: 2450 MHz (2.45 GHz). Tank capacity: 2.8 L, Dimensions: 46.1 cm x 28.0 cm x 37.3 cm.

The microwave reactor was equipped with a stirrer motor and a reflux condenser. Reaction temperature was monitored using a K-type thermocouple connected to an Omron temperature controller. The probe was introduced through the upper access port and positioned in the reaction medium, with the connecting leads electrically insulated. A fiber-optic temperature sensor was not used. Because a metallic thermocouple may perturb the local electromagnetic field and a single-point measurement cannot represent the complete spatial temperature distribution, the reported temperature should be interpreted as the local operational temperature recorded at the probe position rather than as a rigorously validated uniform bulk temperature. A mixture of butanol and coconut oil at butanol-to-oil molar ratios of 6:1–12:1 containing 0.5 wt% NaOH, based on the mass of coconut oil, was processed in the microwave-assisted two-neck flask reactor (Fig. 1) at a selected microwave output of 150 W, 70–110 °C, and reaction times of 1–5 min. After transesterification, 1 % HCl was added to neutralize residual alkaline catalyst and facilitate phase

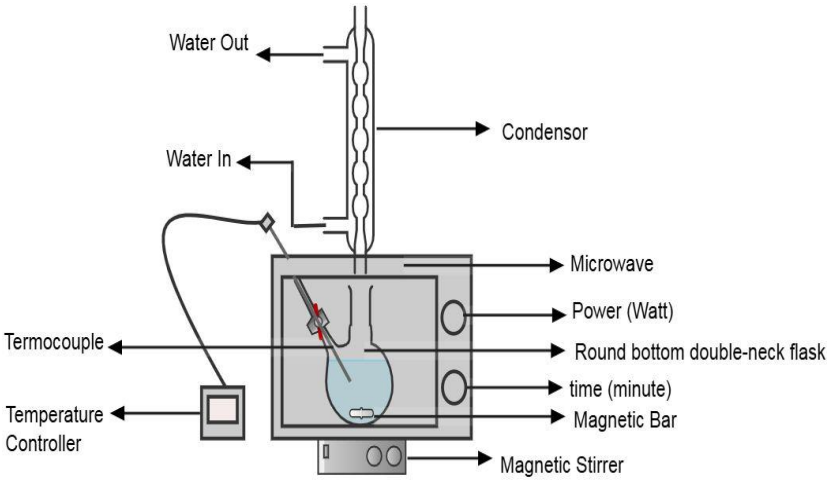


Fig. 1 Experimental set-up of the microwave-assisted biodiesel reactor unit.

separation. A transparent gel-like phase was observed before neutralization; because this phase was not independently characterized, it is not assigned exclusively to soap formation. The neutralized mixture was transferred to a separating funnel, the glycerol-rich phase was removed, and the ester-rich phase was washed with warm distilled water (70–80 °C) at approximately 1.5 times the reaction volume. Excess butanol was subsequently removed by distillation. Butanol recovery efficiency, total process mass loss, and condensate composition were not quantitatively recorded; therefore, a reliable retrospective solvent-recovery or closed overall mass balance cannot be constructed from the available data. The recovered FABE product was subsequently characterized by the selected properties described below.

2.4 Optimization Using Response Surface Methodology (RSM)

Response Surface Methodology (RSM) was employed to efficiently optimize operating parameters while minimizing the number of experimental runs and capturing factor interactions. RSM employs statistical and mathematical techniques to construct predictive models that quantify the influence of independent variables on process outcomes, thereby facilitating the determination of optimal operating parameters (Radojković *et al.*, 2012). In this work, optimization of the microwave-assisted transesterification process was conducted using a FCCD in Design-Expert software (version 13.0). The FCCD configuration positions axial points at the center of each factorial face (coded as ±1), which ensures that experimental conditions remain within a practical and feasible range (Nekkanti *et al.*, 2009). The independent variables investigated were reaction temperature (70–110 °C), reaction time (1–5 min), and butanol-to-oil molar ratio (6:1–12:1), with biodiesel yield designated as the response variable (Table 1). Model adequacy and the significance of each factor were assessed using Analysis of Variance (ANOVA), with evaluation based on F-values, p-values, and the coefficient of determination (R^2) to identify the optimal operating window. Experimental data were fitted to a quadratic model, represented by the generalized form in Equation (1) (Iqbal *et al.*, 2020) to predict the best possible response.

$$Y = \beta_0 + \sum_{i=1}^{k} \beta_i X_i + \sum_{i=1}^{k} \beta_{ii} {X_i}^2 + \sum_{i<j}^{k} \beta_{ij} X_i X_j + \varepsilon \quad (1)$$

Where:

Y = response variable (e.g., yield)
β_0 = intercept
β_i = coefficients for linear terms
β_{ii} = coefficients for quadratic terms
β_{ij} = coefficients for interaction terms
X_i, X_j = variables or factors
ε = error term

2.5 Reaction Kinetics

In biodiesel production, transesterification is the key chemical reaction in which triglycerides are converted into alkyl esters and glycerol through reaction with a short-chain alcohol, such as butanol, in the presence of a catalyst, as represented by Eq. (2):

$$T + 3A \rightarrow 3E + G \quad (2)$$

Here T denotes triglyceride, A alcohol, E alkyl ester, and G glycerol. Kinetic studies have demonstrated that transesterification proceeds through three consecutive and reversible reaction steps involving diglyceride (D) and monoglyceride (M) intermediates (Ezzati *et al.*, 2021):

$$T + A \rightleftharpoons D + E \quad (3)$$

$$D + A \rightleftharpoons M + E \quad (4)$$

$$M + A \rightleftharpoons G + E \quad (5)$$

Based on these reaction pathways, the general rate expression for triglyceride consumption can be expressed as (Andreo-Martínez *et al.*, 2018):

$$-r_T = -\frac{d[T]}{dt} = k_1[T]^m[A]^n \quad (6)$$

where k_1 is the rate constant, m and n are the reaction orders with respect to triglyceride and alcohol concentrations, respectively.

In the present kinetic analysis, butanol was supplied in excess relative to triglyceride and its concentration was treated as approximately constant over the fitted reaction interval. The alcohol-dependent contribution was therefore incorporated into an apparent rate coefficient. This treatment provides a lumped empirical description of conversion and does not establish an elementary molecular reaction order (Mahfud *et al.*, 2018; Souza *et al.*, 2019).

$$-r_T = -\frac{d[T]}{dt} = k_1 . [A]^n . [T]^m$$

Accordingly, the alcohol-dependent term was incorporated into an apparent rate constant, $k_1 . [A]^n = k_1'$, reducing the general rate expression to

$$-\frac{d[T]}{dt} = k_1' . [T]^m$$

For evaluation of the pseudo-first-order model, a first-order dependence on triglyceride concentration (m = 1) was assumed, giving

Table 1.
Experimental factors and their levels.

Parameter	Units	Low	High
Time	minutes	1	5
Temperature	°C	70	110
Ratio		6	12

$$-\frac{d[T]}{dt} = k_1'.[T]^1$$

For the pseudo-first-order representation, a first-order dependence on the changing triglyceride concentration was assumed after incorporating the excess-butanol contribution into the apparent constant. The resulting k_1' is an apparent pseudo-first-order rate constant with units of min^{-1}. This fitted relationship should not be interpreted as evidence of an elementary first-order mechanism.

$$-\frac{d[T]}{dt} = k_1'.[T] \quad (7)$$

The triglyceride concentration at time t can be expressed in terms of conversion X as:

$$[T] = [T]_0\,(1 - X) \quad (8)$$

By simplifying the reaction equation and substituting (8) into (7) :

$$\frac{d\,X}{dt} = k_1'.\,(1 - X) \quad (9)$$

Integration of Eq. (9) yields the following relationship (Hazrat *et al.*, 2022) :

$$\ln(1 - X) = -k_1'.t \quad (10)$$

$k_1' = \min^{-1}, [T]_0 = \text{mol L}^{-1}, [T] = \text{mol L}^{-1}$, where X is triglyceride conversion, t is reaction time (min), k1' is the apparent pseudo-first-order rate constant (min^{-1}), $[T]_0$ is the initial triglyceride concentration, and [T] is the triglyceride concentration at time t.

$k_2' = k_2\,.[A]^n$, In addition to the pseudo-first-order representation, the data were fitted with an apparent pseudo-second-order model with respect to triglyceride concentration. Because butanol was treated as effectively constant owing to its excess, its contribution was incorporated into the apparent second-order coefficient k_2'. Assuming an apparent second-order dependence on triglyceride concentration gives the integrated conversion form $X/(1-X) = k_s\,t$, where $k_s = k_2'\,[T]_o$. The coefficient k_2' has units of L mol^{-1} min^{-1}, whereas the lumped constant k_s has units of min^{-1}. This formulation is an empirical conversion model and should not be interpreted as an elementary overall second-order reaction involving both triglyceride and butanol (Zeng *et al.*, 2017).

$$-r_T = -\frac{d[T]}{dt} = k_2'.[T]^m \quad (11)$$

Integrating Eq. (11) with m = 2 and then, the result of integration:

$$\frac{1}{T} - \frac{1}{T_0} = k_2'\,.t \quad (12)$$

Substitution of equation (8) into (12). Assuming $k_s = [T]_o\,k_2'$, the equation for a pseudo-second-order reaction is :

$$\frac{X}{(1-X)} = k_s.t \quad (13)$$

In this notation, k_2' is the apparent second-order coefficient (L mol^{-1} min^{-1}), $[T]_o$ is the initial triglyceride concentration (mol L^{-1}), and $k_s = k_2'\,[T]_o$ is the lumped pseudo-second-order constant (min^{-1}). These definitions are used consistently in the kinetic interpretation and Arrhenius analysis.

2.6 Product Analysis

The recovered FABE product was characterized in terms of density, kinematic viscosity, flash point, cetane number, and GC–MS compositional profile. The measured density, kinematic viscosity, flash point, and cetane number were compared only with the corresponding SNI 7182:2015 limits for those specific evaluated properties. These measurements do not establish full SNI compliance.

Kinematic viscosity was measured using an Ostwald viscometer by comparing the flow time of the product with that of distilled water to a fixed mark. The process response reported as yield was calculated gravimetrically from the mass of recovered ester-rich product relative to the initial mass of coconut oil, as expressed in Eq. (14). Because standardized quantitative ester-content analysis using a validated GC method with an internal standard was not performed, this response is interpreted as gravimetric product-recovery yield and not as standardized total ester purity or chemical conversion.

$$\boldsymbol{Yield} = \frac{\boldsymbol{m_{bd}\ x\ purity}}{\boldsymbol{m_{co}}}\ \boldsymbol{x\ 100}\ \% \quad (14)$$

where the numerator ($\mathbf{m_{bd}}$) is the mass of recovered ester-rich product (g) and the denominator ($\mathbf{m_{co}}$) is the initial mass of coconut oil (g). The gravimetric recovery does not constitute a closed overall mass balance because solvent-recovery efficiency and total process mass loss were not quantified.

Flash point and cetane number results were obtained from testing conducted at Politeknik Negeri Sriwijaya, Indonesia. The retained study record supports the reported experimental property values; however, detailed instrument-model and test-protocol information should only be stated where it can be verified from the original laboratory report. Accordingly, the present manuscript does not infer or reconstruct undocumented analytical details retrospectively.

2.7 Biodiesel GC-MS Analysis

The chemical composition of fatty acid butyl ester (FABE) was analyzed using a Shimadzu GCMS-QP2010 SE system at the Laboratorium Terpadu of Universitas Islam Indonesia (UII), Yogyakarta. The GC–MS system was equipped with an Rtx-5MS capillary column (5% diphenyl/95 % dimethyl polysiloxane), while helium was used as the carrier gas. Prior to analysis, the sample was diluted in n-hexane, and 0.50 µL was injected into the GC–MS system. Compound identification was performed using WILEY7.LIB spectral database through GCMS solution software.

3. Result and discussion

3.1. Effect of Reaction Temperature on Yield

Temperature is a critical operational parameter that governs the transesterification process by influencing reaction kinetics, mass transfer, and overall conversion efficiency. In conventional heating systems, achieving and maintaining the desired temperature is often time-consuming and energy-intensive. In contrast, microwave irradiation provides rapid and volumetric heating, enabling faster energy transfer to reactants and more uniform temperature distribution within the reaction medium.

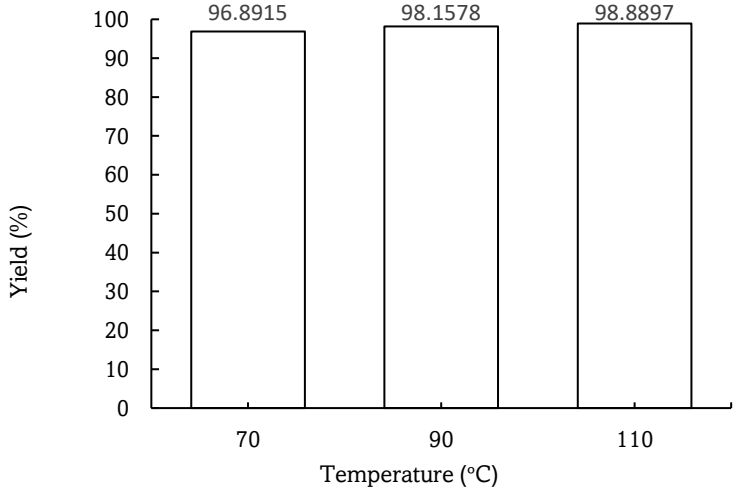


Fig. 2 Effect of reaction temperature on biodiesel yield.

Transesterification experiments were conducted using 0.5 wt% NaOH catalyst with sufficient residence time to ensure effective interaction between triglycerides and butanol, thereby promoting conversion to fatty acid butyl esters (FABE). Catalyst concentration governs the availability of hydroxide ions that initiate nucleophilic attack on triglyceride molecules. Although higher catalyst loadings can accelerate reaction rates, excessive amounts may induce soap formation, leading to reduced ester yield and impaired phase (Mahfud *et al.*, 2025; Suryanto *et al.*, 2015). Under microwave-assisted conditions, enhanced molecular interactions and accelerated kinetics enable biodiesel production within significantly shorter reaction times. However, process performance remains strongly dependent on operating temperature. An optimal temperature range is required to supply sufficient activation energy for transesterification while avoiding undesirable side reactions or thermal degradation.

Fig. 2 shows the relationship between reaction temperature and butyl ester yield under microwave-assisted conditions. Experiments were conducted at temperatures of 70 °C, 90 °C, and 110 °C, while maintaining a reaction time of 3 min, NaOH loading of 0.5 wt.%, and an butanol-to-oil molar ratio of 12:1. The results demonstrate a clear dependence of biodiesel yield on temperature, highlighting the existence of an optimal operating window that maximizes conversion efficiency and supports intensified biodiesel production.

As shown in Fig. 2, biodiesel yield increased with rising reaction temperature, reaching values of 96.89 %, 98.16 %, and 98.89 % at 70 °C, 90 °C, and 110 °C, respectively. This positive temperature dependence can be attributed to enhanced molecular motion and reduced oil viscosity at elevated temperatures, which improve mass transfer between triglycerides and alcohol. Consequently, collision frequency between reactant molecules increases, accelerating ester formation.

Nevertheless, the incremental improvement in yield from 90 °C to 110 °C is relatively modest compared with the increase observed between 70 °C and 90 °C. This trend indicates that the reaction approaches equilibrium at higher temperatures,

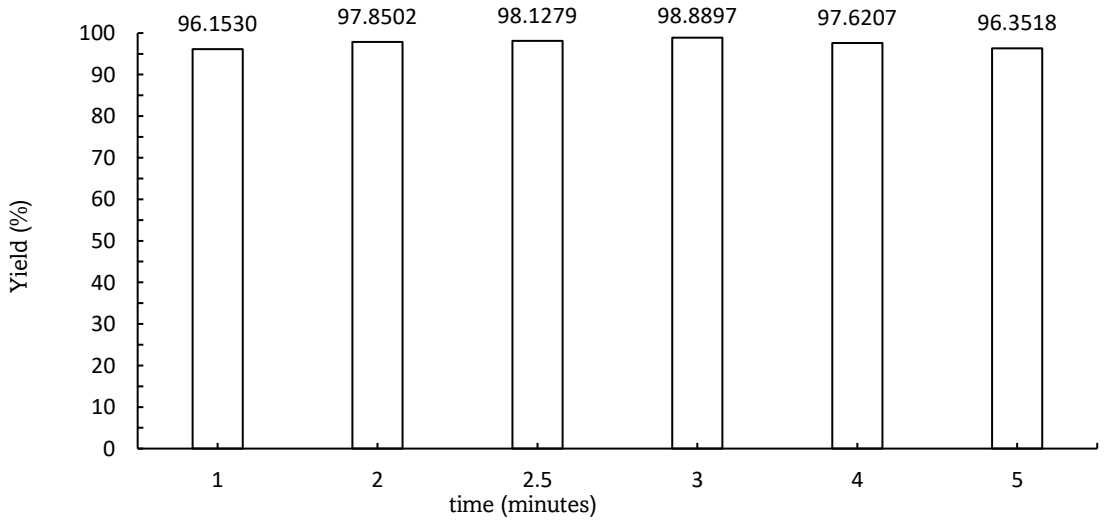


Fig. 3 Effect of reaction time on biodiesel yield.

beyond which further heating provides diminishing benefits. Excessively high temperatures may also promote alcohol evaporation and side reactions, such as saponification, which complicate downstream separation and purification. Similar observations have been reported by Kurczyński *et al.* (2022), who demonstrated that optimal temperature control is essential for maximizing butyl ester yields while preserving fuel quality

Excessive temperatures may lead to undesirable effects such as alcohol evaporation, which reduces the effective concentration of the reactant, and soap formation due to side reactions, which complicates product separation and purification. Similarly, Kurczyński *et al.* (2022), reported that butyl ester yields are maximized under carefully controlled temperature conditions, with yields approaching 99 % for animal fat butyl esters. However, excessive temperatures can negatively impact product quality and yield.

3.2. Effect of Reaction Time on Biodiesel Yield

Microwave-assisted transesterification is recognized for its ability to deliver rapid volumetric heating, enhance energy efficiency, and significantly reduce reaction duration. Unlike conventional heating, microwave irradiation directly couples with polar molecules, enabling uniform and intensified heating throughout the reaction medium and thereby reducing reaction time while maintaining high conversion efficiency. Under fixed conditions (110 °C, 0.5 wt.% NaOH, 12:1 molar ratio), the relationship between reaction time (1–5 min) and butyl ester yield is shown in Fig. 3. The yield rises steeply at first, maximizing at approximately 3 minutes. This rapid increase demonstrates that high FABE yield can be achieved within a very short reaction time under the investigated microwave-assisted conditions. Beyond 3–4 min, the yield exhibits only marginal changes, indicating that the reaction has reached equilibrium under the studied conditions.

The rapid conversion observed under the investigated microwave-assisted butanolysis conditions enabled high FABE yields within a short reaction time. This observation is consistent with previous studies reporting short reaction times for microwave-assisted biodiesel production (Kurniati *et al.*, 2019; Koech *et al.*, 2020; Hsiao *et al.*, 2021). These findings confirm that prolonged reaction times are unnecessary and may even be undesirable, as they offer limited additional benefit once equilibrium is achieved.

3.3. Effect of Reactant Ratio on Biodiesel Yield

An excess of butanol is required to favor ester formation in transesterification, making the butanol-to-oil molar ratio a fundamental variable. This parameter is especially significant under microwave-assisted conditions, where reaction kinetics and mass transfer are substantially enhanced. The influence of the butanol-to-oil molar ratio on biodiesel yield is presented in Fig. 4. Under fixed conditions of 110 °C, 3 min, and 0.5 wt.% NaOH catalyst, increasing the molar ratio from 6:1 to 12:1 resulted in a progressive increase in yield from 93.32 % to 98.89 %. The highest yield was attained at a 12:1 ratio. This increase demonstrates that excess butanol effectively drives the reaction equilibrium toward ester production, enhancing overall conversion (Kannan *et al.*, 2024; Kumar & Sethy, 2015).

The improvement in yield with increasing molar ratio can be attributed to the greater availability of alcohol molecules, which accelerates transesterification kinetics and reduces the likelihood of unreacted triglycerides. However, the incremental gain observed between ratios of 9:1 and 12:1 is smaller than that between 6:1 and 9:1, indicating that the reaction approaches equilibrium at higher alcohol excess. Beyond this range, further increases in butanol concentration are expected to provide marginal yield enhancement while increasing operational complexity, particularly in terms of separation and energy demand for alcohol recovery.

The data presented in Figures 2–4 are individual experimental observations from single runs at each investigated condition. Independent replication was not performed for these single-factor screening experiments; therefore, standard-deviation error bars or confidence intervals cannot be reconstructed and are not reported. These trends should be interpreted descriptively. Statistical error estimation for the FCCD model is restricted to the replicated center-point information contained in that design.

In the NaOH-catalyzed butanolysis system, phase behavior during reaction and work-up may be influenced by alkaline species, water, glycerol, residual fatty acids, hydrolysis/saponification reactions, surfactant-like intermediates, and the limited miscibility of polar and non-polar components. A transparent gel-like phase was observed during post-reaction handling before neutralization. Because this material was not independently characterized by FTIR, NMR, or another phase-specific method, its composition cannot be attributed exclusively to soap formation. Addition of 1 % HCl

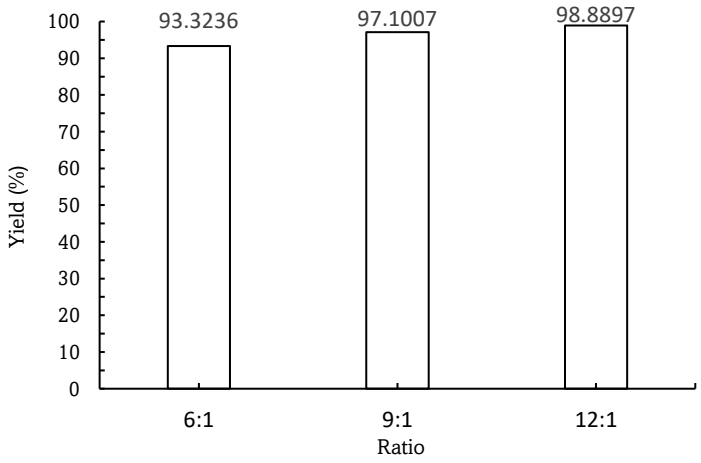


Fig. 4 Effect of butanol-to-oil molar ratio on biodiesel yield.

Table 2.
Regression models for predicting biodiesel yield.

Source	Sequential p-value	Lack of Fit p-value	Adjusted R^2	Predicted R^2	
Linear	0.0007	0.0291	0.5770	0.3462	
2FI	0.6732	0.0204	0.5356	-1.2825	
Quadratic	< 0.0001	0.9675	0.9457	0.9309	Suggested
Cubic	0.9872	0.5033	0.9138	-2.1798	Aliased

after transesterification was used operationally to neutralize residual alkaline catalyst and facilitate phase separation. The observation is therefore discussed as plausible composition-dependent phase behavior rather than as proof of a unique gel-formation mechanism.

Microwave heating plays a key role in achieving high biodiesel yields within a short reaction time. Unlike conventional heating, microwave irradiation enables rapid and uniform energy transfer through dipole rotation and ionic conduction, enhancing molecular interactions and reducing system viscosity. These effects improve mass transfer and reaction kinetics, allowing near-complete conversion to be achieved within 3 min at 110 °C (Milano *et al.*, 2024). Overall, high FABE yields were obtained using excess butanol under the investigated microwave-assisted reaction conditions.

3.4. Integrated FCCD Optimization, Response Surface Analysis, and Model Validation

3.4.1 Experimental Design and Variable Selection

The experimental design was based on a three-factor face-centered central composite design (FCCD) with reaction time (A: 1–5 min), temperature (B: 70–110 °C), and butanol-to-oil molar ratio (C: 6:1–12:1). The 20-run design comprised 8 factorial points, 6 face-centered axial points, and 6 center-point runs. The center points provide the replicated observations available within the FCCD for estimation of pure error and assessment of model adequacy; they should not be interpreted as replication of the separate single-factor screening experiments. The complete FCCD matrix, including actual factor levels, experimental yields, model-predicted yields, and residuals, is presented in Table 3. Linear, two-factor interaction (2FI), quadratic, and cubic models were evaluated using sequential and lack-of-fit p-values, adjusted R^2, and predicted R^2. A total of 20 experimental runs were generated using a three-factor face-centered central composite design (FCCD), comprising 8 factorial points, 6 face-centered axial points, and 6 replicated center points. The complete experimental design matrix, together with the experimental and model-predicted FABE yields, is presented in Table 3. As shown in Table 3, the predicted FABE yields were generally close to the experimental values across the investigated design space, indicating good agreement between the quadratic model and the experimental data. The relatively small residuals further support the adequacy of the developed regression model for predicting FABE yield within the studied factor ranges.

3.4.2 Model Selection and Statistical Validation

The biodiesel yield was modeled using Design-Expert software (v. 13) by evaluating linear, two-factor interaction (2FI), quadratic, and cubic regression models. Model selection relied on key statistical indicators: sequential p-value, lack-of-fit p-value, adjusted R^2, and predicted R^2. The quadratic model was selected as optimal, demonstrating a highly significant sequential p-value (< 0.0001) and a non-significant lack-of-fit p-value (0.9675 > 0.05). This indicates the model provides a statistically significant improvement over simpler models and fits the experimental data adequately, consistent with

Table 3.
Face-centered central composite design (FCCD) matrix and comparison of experimental and predicted FABE yields.

Run	Design Point	Time (min)	Temperature (°C)	Butanol to Oil Ratio	Experimental Yield	Predicted Yield	Residual
1	1	1	70	6:1	85.6000	85.7859	-0.1859
2	1	1	110	6:1	87.6600	87.6023	0.0577
3	-1	3	90	12:1	98.1578	97.8217	0.3361
4	-1	1	90	9:1	93.3759	93.0612	0.3147
5	1	1	70	12:1	94.8003	94.6701	0.1302
6	0	3	90	9:1	95.2404	96.1186	-0.8782
7	1	5	70	12:1	94.7607	94.9185	-0.1578
8	1	5	110	12:1	96.4456	96.3613	0.0843
9	-1	3	110	9:1	97.1007	96.7214	0.3793
10	0	3	90	9:1	95.7699	96.1186	-0.3487
11	1	1	110	12:1	96.1530	96.4409	-0.2879
12	-1	3	70	9:1	95.2206	95.0918	0.1288
13	0	3	90	9:1	96.4973	96.1186	0.3787
14	0	3	90	9:1	95.2553	96.1186	-0.8633
15	-1	3	90	6:1	91.1402	90.9667	0.1735
16	0	3	90	9:1	95.2553	96.1186	-0.8633
17	-1	5	90	9:1	95.3435	95.1520	0.1915
18	1	5	110	6:1	91.3040	91.5355	-0.2315
19	0	3	90	9:1	97.7937	96.1186	1.6751
20	1	5	70	6:1	90.2329	90.0471	0.1858

Note: The 20-run FCCD contains 8 factorial points, 6 face-centered axial points, and 6 center-point runs. Center-point replication is used for model error assessment and does not imply replication of the separate single-factor screening experiments.

established modeling practices (Angassa *et al.*, 2023; Okpala & Dibia, 2025).

The suitability of the model is further supported by its high adjusted R^2 (0.9457), demonstrating strong explanatory power, and its predicted R^2 (0.9309), indicating robust predictive capability and a close correspondence between the experimental and predicted values. In contrast, the linear model showed limited performance, with a low adjusted R^2 of 0.5770 and poor predictive reliability, reflecting its inability to capture the variability of the response.

Although the cubic model exhibited a relatively high adjusted R^2 value (0.9138), its predicted R^2 was negative (−2.1798), and the model was aliased, indicating that some regression terms could not be independently estimated due to confounding effects. Consequently, the cubic model was deemed unsuitable for reliable interpretation and prediction. Based on the selected quadratic model, the resulting simulation and optimization of biodiesel (butyl ester) yield are presented in Fig.5, with corresponding numerical results summarized in Table 3.

3.4.3 Effect Ranking and Pareto Analysis

Fig. 5 presents the Pareto chart of standardized effects, showing the relative impact of independent variables and their interactions on FABE yield. The analysis, derived from an FCCD optimization of reaction time (A), temperature (B), and reactant ratio (C), applied a significance level of $\alpha = 0.05$ (critical t-value = 2.23). The results indicate that the butanol-to-oil molar ratio (C) exerts the strongest effect on yield. Significant contributions from the linear and quadratic terms of reaction time (A, A^2), along with the quadratic effect of the reactant ratio (C^2) and the AC interaction, reveal an optimum in the region characterized by high alcohol excess and short reaction durations (approximately 3 min). In contrast, reaction temperature (B) exhibits a moderate effect within the investigated range of 70–110 °C. These results suggest that process optimization should primarily focus on controlling the reactant ratio and reaction time, with temperature serving as a secondary tuning parameter to ensure high conversion and stable operation.

3.4.4 ANOVA Analysis for butyl ester optimization

As shown in Table 4, ANOVA indicates the quadratic model provides a statistically significant fit for the yield data (model F-value = 37.76, $p < 0.0001$; lack-of-fit $p = 0.9675$). Factor significance analysis reveals the butanol-to-oil molar ratio (C) as the predominant variable ($F = 196.18$, $p < 0.0001$), with reaction time (A) and temperature (B) also contributing significantly. This demonstrates that stoichiometric excess is the primary driver of transesterification completion, while sufficient reaction time is necessary to maximize conversion. Temperature, although statistically significant, showed a smaller effect than the butanol-to-oil molar ratio within the studied range.

Significant quadratic effects were observed for reaction time (A^2, $p = 0.0016$) and reactant ratio (C^2, $p = 0.0042$), whereas the quadratic term for temperature (B^2) was not significant ($p = 0.6595$). In addition, the interaction between reaction time and reactant ratio (AC) was statistically significant ($p = 0.0044$), while AB and BC interactions were negligible. These findings confirm the presence of an optimal operating region governed mainly by the combined effects of reaction time and molar ratio rather than simple linear trends.

The observed trends further indicate the existence of an optimal reaction duration within the short time window of 1–5 min. Beyond this range, prolonged microwave irradiation may promote undesirable side reactions or thermal degradation due to excessive localized heating (Cercado *et al.*, 2018). This behavior is consistent with previous studies reporting that excessive reaction times can reduce biodiesel yield as a result of unfavorable secondary reactions (Refaat *et al.*, 2008).

In contrast, the two-factor interactions involving temperature (B^2, AB, and BC) are statistically insignificant within the examined temperature range (70–110 °C). This observation is characteristic of microwave-assisted transesterification systems, where rapid and efficient dielectric heating promotes uniform temperature distribution throughout the reaction medium.

The dominance of the quadratic terms and the AC interaction suggests that excessively long reaction times or very high alcohol ratios may lead to diminishing returns or promote undesirable side reactions. Therefore, process optimization

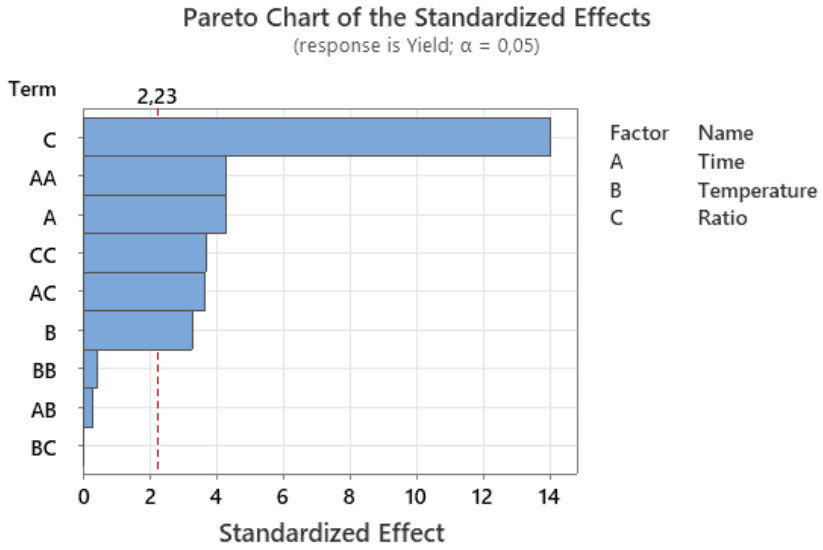


Fig. 5 Pareto chart of standardized effects for FABE yield optimization.

Table 4.
Analysis of variance (ANOVA) for the FCCD regression model of FABE yield.

Source	Sum of Squares	df	Mean Square	F-value	p-value	
Model	204.76	9	22.75	37.76	< 0.0001	significant
A-Time	11.02	1	11.02	18.29	0.0016	
B-Temperature	6.48	1	6.48	10.75	0.0083	
C-Ratio	118.20	1	118.20	196.18	< 0.0001	
AB	0.0539	1	0.0539	0.0895	0.7710	
AC	8.05	1	8.05	13.36	0.0044	
BC	0.0011	1	0.0011	0.0018	0.9669	
A^2	11.15	1	11.15	18.50	0.0016	
B^2	0.1242	1	0.1242	0.2062	0.6595	
C^2	8.18	1	8.18	13.57	0.0042	
Residual	6.03	10	0.6025			
Lack of Fit	0.8273	5	0.1655	0.1592	0.9675	not significant
Pure Error	5.20	5	1.04			
Cor Total	210.78	19				

should focus on identifying the optimal balance between reaction time and reactant ratio while maintaining temperature within a moderate range to ensure efficient energy utilization and stable operation.

Based on the ANOVA results, an empirical optimization equation for biodiesel (butyl ester) yield was developed using FCCD. The resulting quadratic model, expressed as Equation (15), describes the combined effects of the significant variables on biodiesel production.

$$Yield\ (\%) = 51.042 + 5.2343A + 0.144B + 5.113C - 0.0021AB - 0.167AC - 0.00019BC - 0.503A^2 - 0.00053B^2 - 0.192C^2 \quad (15)$$

where A is reaction time, B is temperature, and C is the butanol-to-oil molar ratio. Equation (15) is expressed in actual factor units, not coded units. In a quadratic response-surface model, positive linear coefficients may coexist with negative quadratic and interaction terms; the response is determined by the complete polynomial rather than by any coefficient in isolation. Model validity is therefore assessed from the full fitted equation together with ANOVA, residual diagnostics, predicted-versus-experimental agreement, and optimization results.

The fit statistics (Table 5) presented affirm the statistical reliability and predictive power of the RSM model employed for optimizing yield. The concise relationship between prediction accuracy and variability, coupled with robust adequacy measures, establishes the validity of this approach in engineering applications.

Table 5.
Model fitting statistics for the FCCD regression model of FABE yield.

Fit Statistic	**Result**
Std. Dev.	0.7762
Mean	94,16
C.V. %	0.8244
R^2	0.9714
Adjusted R^2	0.9457
Predicted R^2	0.9309
Adeq Precision	21.9609

The fit statistics indicate that the developed model was statistically adequate for optimization using response surface methodology (RSM). The Standard Deviation of 0.7762 implies low variability in the predictions of the model when compared to the mean yield of 94.16 %, which contributes to the reliability of the obtained predictions (Mohammed *et al.*, 2021). The coefficient of variation (C.V. = 0.824 %) is well below 10 %, which is generally considered acceptable for experimental models, confirming high precision and consistency (Montgomery, 2013).

Key metrics, such as R^2 and Adjusted R^2, reveal the model's strength in explaining variability in the response variable. With R^2 reported at 0.9714 and Adjusted R^2 at 0.9457, it is evident that over 97 % of the variability in biodiesel yield can be elucidated by the model. The close agreement between the Predicted R^2 of 0.9309 and the Adjusted R^2 suggests robustness in the model's predictive capability, indicating that it has not been overfitted and can generalize well to unseen data (Betiku *et al.*, 2015). A difference of less than 0.2 between these two metrics indicates that the predictions remain reliable across the design space, thus affirming their validity (Chen & Qi, 2023).

Furthermore, the Adequate Precision value of 21.9609 significantly surpasses the minimum threshold of 4, indicating a strong signal-to-noise ratio. This metric is crucial as it suggests that the model possesses sufficient signal strength for statistically sound decision-making in optimization scenarios. The associated high Adequate Precision affirms the model's effectiveness in navigating the complex interactions inherent in the RSM framework, further enhancing its applicability in optimization tasks related to biodiesel production (Zabaruddin *et al.*, 2020).

3.4.5 Response Surface and Contour Plot Analysis

RSM is established as a robust statistical tool for optimizing the conditions that affect biodiesel yields, allowing researchers to delineate the impacts of multiple variables simultaneously while limiting experimental runs (Babaki *et al.*, 2017; Yamin *et al.*, 2024). This study investigates the main effects and interactions of each parameter on the yield of biodiesel (butyl ester) through the use of contour and surface

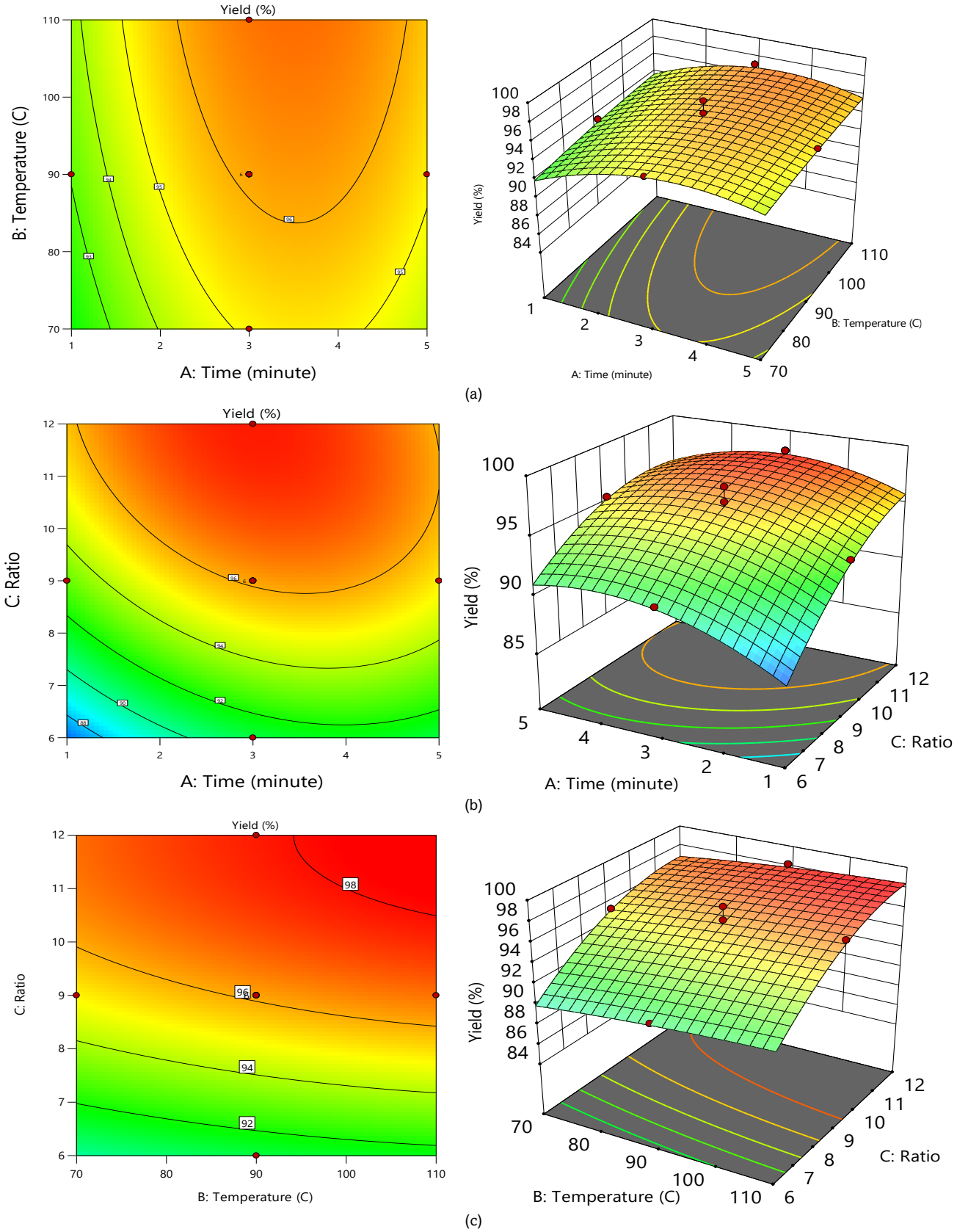


Fig 6. Contour and three-dimensional response surface plots for FABE yield as a function of: (a) reaction time and temperature; (b) reaction time and reactant molar ratio; and (c) temperature and reactant molar ratio.

plots. These graphical representations illustrate the regression equation by showing the relationship between two variables. The plots are derived from the quadratic model applied in the analysis. These graphical representations of data, including the contour plot and 3D surface plot highlighted by Fig. 6a – 6c, engage prominently with the variables of time (minutes),

temperature (Celsius), and reactant ratio to elucidate their interactions with biodiesel yield (%).

The contour plot illustrates the interaction between reaction time (minutes), temperature (°C), reactant ratio, and their combined influence on biodiesel (butyl ester) yield. Utilizing a gradient color scale, the plot visually communicates yield variations, with blue regions representing lower yields (as low as 85.6 %) and red regions indicating higher yields (up to 98.156 %). This visualization serves as a powerful tool for process optimization, enabling a clear understanding of how these two independent variables interact to affect the response variable yield (%) (Renita *et al.*, 2014).

The central area of the plot, dominated by red hues, suggests that optimal yields are achieved at moderate levels of both temperature and reaction time, highlighting a specific zone favorable for biodiesel synthesis (Chin *et al.*, 2009). In contrast, the outer regions shaded in blue reflect suboptimal conditions, where the yield is significantly reduced. These findings reinforce the importance of precise control over reaction parameters, particularly temperature and time, to maximize biodiesel output (Doori *et al.*, 2022; Roushdy, 2022). Moreover, the contour plot supports the statistical conclusions derived from the quadratic regression model used in the study. It enhances the interpretation of experimental design by revealing the nature of interaction effects between the key variables. The significance of these interactions underscores the value of employing RSM in process optimization, as it allows researchers to identify ideal operational conditions within experimental constraints (Renita *et al.*, 2014; Özgur *et al.*, 2017).

The contour plot contributes to a deeper understanding of factor interactions and serves as a guide for future experimental designs aimed at improving biodiesel production efficiency. This approach not only enhances yield outcomes but also supports the broader goal of advancing sustainable energy technologies through biodiesel synthesis (Aracil *et al.*, 2010; Setiadji *et al.*, 2018). As depicted in the 3D surface plot, the interplay between reaction time and temperature can be visually interpreted, offering insights into maximum yields under specific conditions (Babaki *et al.*, 2017). The color-coded regions assist in determining the optimal and suboptimal parameters, where blue indicates lower yields and red highlights higher yields. The axes are labeled as A (Time), B (Temperature), C (Ratio) and Yield (%), corresponding to the experimental factors and response. The plot serves not only as a validation of the predictions made by the regression model but also as a framework for assessing the practical implications on biodiesel. The strength of RSM lies in its ability to reflect complex relationships and interactions, tracking how varying the temperature and time can enhance or diminish yield, thus supporting claims of optimal biodiesel production conditions (Kumar *et al.*, 2021).

Design points are plotted on the surface, with red dots indicating observations above the predicted surface and white dots representing those below it. This helps in assessing the model's fit and identifying any deviations between predicted and actual values. Specifically, the interaction between these parameters is paramount for understanding how adjustments impact the biodiesel synthesis process, underlining RSM's significance in identifying the best processing conditions (Anwar *et al.*, 2018; Niju *et al.*, 2019).

The plot reveals that yield increases with temperature up to a certain point, and time also plays a significant role in maximizing the response. This graphical representation supports the statistical findings and aids in identifying the optimal conditions for achieving the highest yield. The graphical representations of data (like the one presented) not only present a user-friendly understanding of complex mathematical models but also exhibit the model's effectiveness through the high predictive accuracy indicated by R^2 values close to unity, as stated in various studies (Khadivi *et al.*, 2025; Soliman *et al.*, 2024)

The design points indicated upon the surface plot further facilitate the evaluation of model fit and deviation analysis between actual observations and predicted values. This enables a rigorous statistical exploration of the biodiesel production dynamics, affirming RSM's role in successful operational implementations of biodiesel synthesis through robust statistical methodologies (Mohanraj *et al.*, 2022; Maheswaran & Uthranarayan, 2022).

3.4.6 Model Adequacy

The adequacy and predictive performance of the developed model were evaluated by comparing the predicted and experimental results and by examining the diagnostic plots presented in Figs. 7 and 8. The normality of the residuals, an

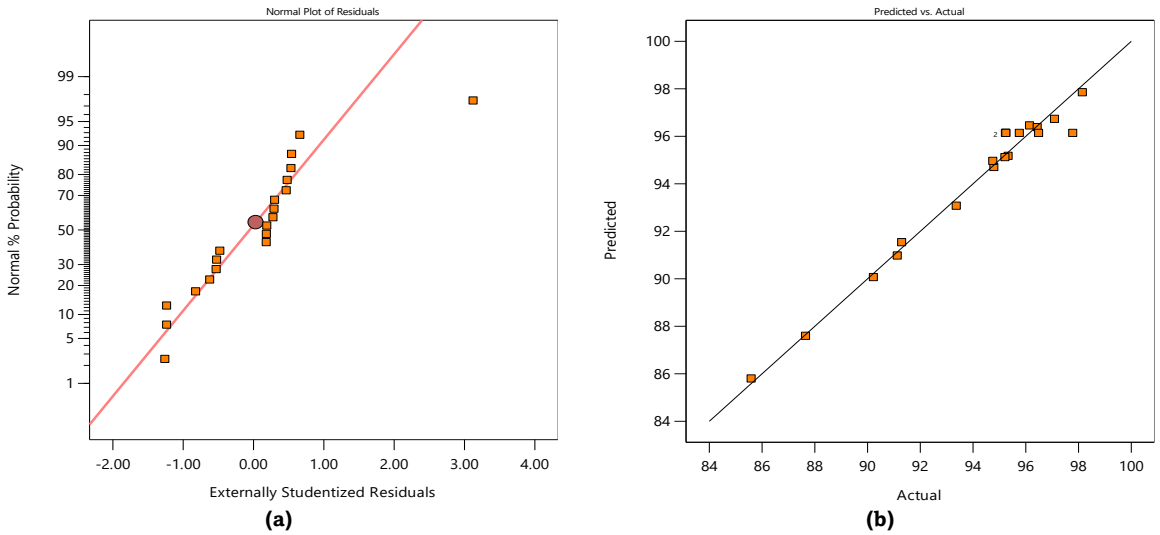


Fig. 7 Diagnostic plots for the FCCD regression model of FABE yield: (a) normal probability plot of residuals and (b) predicted versus actual values

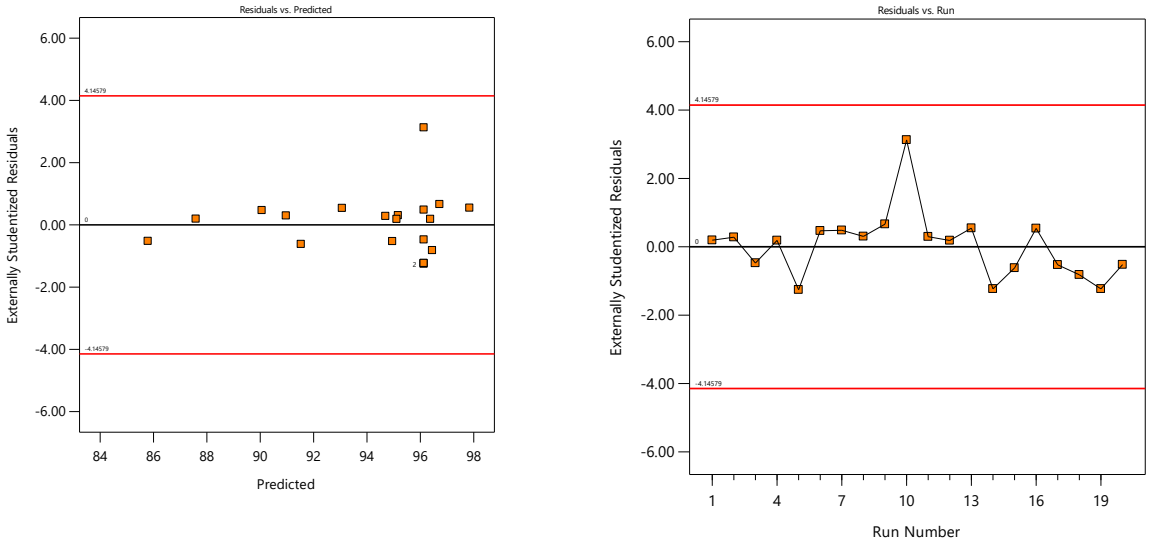


Fig. 8 Residual diagnostic plots for the FCCD regression model of FABE yield: (a) residuals versus predicted values and (b) residuals versus experimental run order.

important assumption in regression analysis, was assessed using the normal probability plot shown in Fig. 7a. The plot presents the externally studentized residuals against the normal percentage probability, with data points following the reference line indicating an approximately normal distribution of the residuals.

The data points are generally distributed close to the reference line, indicating that the residuals approximately follow a normal distribution. No pronounced systematic deviation from the reference line is observed, suggesting the absence of substantial departures from normality. These results support the suitability of the regression model for statistical interpretation and prediction within the investigated experimental domain.

The predictive performance of the model was further evaluated using the predicted versus actual plot (Fig. 7b). The data points are closely distributed around the diagonal reference line, demonstrating good agreement between the predicted and experimental FABE yields. This agreement, together with the high coefficient of determination (R^2) and adequate precision obtained from the statistical analysis, indicates that the model provides satisfactory predictive performance within the investigated design space.

Model assumptions were further examined using the residuals versus predicted values plot (Fig. 8a), in which the externally studentized residuals are plotted against the predicted FABE yields. The residuals are randomly scattered around the zero line without an apparent systematic pattern, supporting the assumptions of constant variance and an appropriate model form. Moreover, no residuals exceed the ±4.14579 diagnostic limits shown in the plot, indicating that no extreme residuals were detected based on these limits. The residuals versus run plot (Fig. 8b) was used to evaluate the randomness and consistency of the residuals throughout the experimental sequence. In this plot, the externally studentized residuals are presented as a function of the experimental run order. As shown in Fig. 8b, the residuals fluctuate randomly around the zero line without an apparent trend or systematic pattern, and none exceed the ±4.14579 diagnostic limits. The absence of a clear run-order-dependent pattern suggests that systematic drift or other sequence-related effects were not evident during the experiments. Collectively, the diagnostic plots in Figs. 7 and 8 support the adequacy, stability, and predictive reliability of the FCCD regression model for describing FABE yield within the investigated design space.

3.4.7. Optimization and Determination of Optimal Conditions

The optimal values of the variables, obtained through FCCD optimization, are presented in Table 6. The optimization of biodiesel yield using FCCD framework is a well-established approach in chemical engineering, offering significant advantages for systematically exploring process variables and their interactions. Originally developed by Box and Wilson, FCCD has been widely adopted because it enables the development of a second-order (quadratic) response model without requiring a full three-level factorial design (Njoku & Otisi, 2023; Verdooren, 2017). This feature is particularly advantageous when minimizing experimental runs is critical, as it allows maximum information to be obtained from a limited number of data, thereby improving optimization efficiency (Çira *et al.*, 2016).

In the present study, FCCD-based optimization identified optimal operating conditions at a reaction time of 2.758 min, a temperature of 108.303 °C, and a reactant ratio of 11.357, resulting in a predicted biodiesel yield of 98.266 % with a composite desirability value of 1. The desirability function plays a central role in RSM by transforming multiple response criteria into a single scalar metric, where values approaching unity indicate a higher likelihood of achieving optimal performance (Czyrski & Jarzebski, 2020). Experimental validation conducted under the predicted optimum conditions produced an actual FABE yield of 98.8897 %, which was in close agreement with the model-predicted value of 98.266 %. This agreement supports the predictive capability of the FCCD model within the investigated design space and confirms its suitability for optimizing the microwave-assisted FABE production process.

Research has demonstrated that similar optimization frameworks employing have been effective in various applications beyond biodiesel using microwave-assisted. For example, research involving Chlorella sp. optimized various parameters using FCCD to achieve biodiesel yields potentially around 99 % by carefully tuning microwave power and other variables, underscoring the effectiveness of this design in

Table 6.
Optimal reaction conditions and validation of the predicted FABE yield.

Solution	Time (minutes)	Temperature (C)	Reactant Ratio	Yield (%) Fit	Composite Desirability
1	2.758	108.303	11.357	98.266	1

elucidating the interaction effects between different operational conditions (Mahfud *et al.*, 2020; Qadariyah *et al.*, 2021).

The integration of RSM and FCCD occupies a pivotal role in the optimization of biodiesel processes, demonstrating a high degree of efficacy in predicting and achieving desirable outcomes (Chakraborty *et al.*, 2014, 2015; Chakraborty & Bepari, 2012). This framework not only reduces the experimental burden but significantly enhances the informative nature of the optimization process, confirming its validity in practical applications within the field of biodiesel production and beyond.

3.5 Kinetics of Butyl Ester Transesterification Reaction

The reaction kinetics were analyzed using two models, namely the pseudo-first-order model (Equation 10) and the pseudo-second-order model (Equation 13), over a temperature range of 70–110 °C and butanol-to-oil ratios of 6:1–12:1. The rate constant (k) increased systematically with both temperature and molar ratio for both models, confirming the role of thermal energy and alcohol availability in accelerating the transesterification reaction. The results are shown in Table 7.

Based on Table 7, the pseudo-second-order kinetic model provided a better fit to the experimental data, with a higher average coefficient of determination (R^2 = 0.974) compared to the pseudo-first-order model (R^2 = 0.935). The superior fit of the pseudo-second-order model should be interpreted as an apparent or lumped kinetic representation of triglyceride conversion under microwave-assisted conditions rather than as evidence of an elementary second-order reaction involving both triglyceride and butanol. n-Butanol has a water solubility of approximately 73 g L^{-1} at 25 °C and remains partially miscible with aqueous phases while exhibiting good solubility in oils and organic compounds. Consequently, its mixture with nonpolar coconut oil, particularly in the presence of a catalyst or trace water, tends to form a biphasic system consisting of butanol-rich and oil-rich phases. The better fit obtained with the pseudo-second-order model should therefore be regarded as an apparent or lumped description of triglyceride conversion under the investigated conditions. It does not imply an elementary second-order reaction involving both triglyceride and butanol, because the excess butanol concentration was incorporated into the apparent rate coefficient. This behavior supports the applicability of a pseudo-second-order kinetic model rather than a pseudo-first-order approximation.

Using the kinetic rate constants obtained at different temperatures (Table 7) and correlating them with the Arrhenius equation, the apparent activation energy (E_a,app) and the pre-exponential factor (A) were subsequently determined as shown in Table 8. The Arrhenius analysis yielded apparent activation energies (E_a,app) of 5.0, 8.1, and 22.5 kJ mol^{-1} at butanol-to-oil molar ratios of 6:1, 9:1, and 12:1, respectively. The increase in (E_a,app) with increasing butanol-to-oil ratio should not be interpreted as an increase in the intrinsic activation energy barrier of the transesterification reaction. Rather, these values were derived from apparent pseudo-second-order rate constants obtained under different mixture compositions and therefore may reflect combined contributions from chemical kinetics, phase behavior, alcohol–oil partitioning, interfacial mass-transfer characteristics, and uncertainty associated with the Arrhenius fitting. The corresponding pre-exponential factor ((A)) also increased with the butanol-to-oil ratio; however, because (A) was derived from the same apparent kinetic model, its variation should likewise be interpreted as an apparent kinetic parameter rather than solely as a direct measure of molecular collision frequency. The obtained (E_a,app) values of 5–23 kJ mol^{-1} fall within the range reported for biodiesel transesterification systems (Yao *et al.*, 2024). The present data are insufficient to uniquely distinguish among the contributions of intrinsic reaction kinetics, phase-equilibrium effects, mass transfer, and regression uncertainty to the observed dependence on the ratio.

Table 7.
Apparent kinetic constants for pseudo-first-order and pseudo-second-order models at various butanol-to-oil molar ratios and temperatures

Ratio	T	k1' (min^{-1})	R^2	ks (min^{-1})	R^2
6:1	70	0.962	0.9406	3.8250	0.9835
	90	0.992	0.9389	4.1071	0.9823
	110	1.0315	0.9408	4.5874	0.9823
9:1	70	1.2762	0.9161	8.5105	0.9364
	90	1.3272	0.9353	9.6888	0.9887
	110	1.3945	0.9249	11.431	0.9742
12:1	70	1.3853	0.9268	11.146	0.9783
	90	1.4959	0.9385	15.301	0.9648
	110	1.6980	0.9503	25.396	0.9763

Table 8.

Arrhenius Equations and Apparent Kinetic Parameters at Various Butanol-to-Oil Molar Ratios

Ratio	Arrhenius Equation	$E_{a,app}$ (kJ/mol)	A
6:1	ln k = 3.10 − 5015/(RT)	5.0	22.3
9:1	ln k = 4.98 − 8100/(RT)	8.1	1.45×10^{2}
12:1	ln k = 10.31 − 22 510/(RT)	22.5	3.0×10^{4}

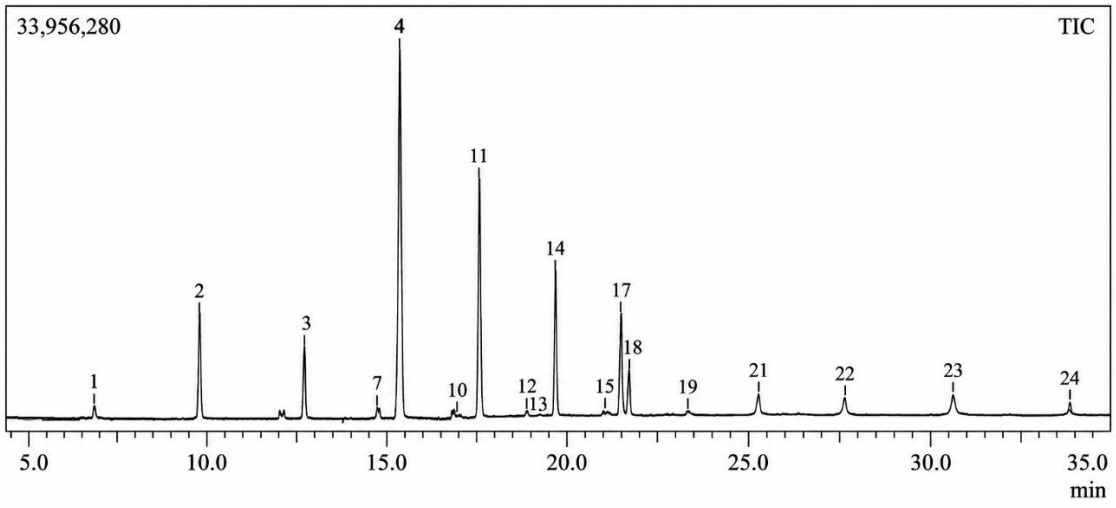


Fig. 9 GC-MS result of butyl ester obtained

3.6. Comparison of Selected FABE Properties with SNI 7182:2015

The measured density, kinematic viscosity, flash point, and cetane number were compared with the corresponding limits in SNI 7182:2015 (Badan Standardisasi Nasional, 2015). Density at 40 °C was 0.850 g cm^{-3} and kinematic viscosity was 3.188 cSt; these values fall within the corresponding limits for those parameters.

The reported flash point and cetane number were 103.4 °C and 57.1, respectively, and were within the corresponding SNI limits for these evaluated properties. These results must not be interpreted as demonstrating full compliance with SNI 7182:2015 (Table 9). Other mandatory quality parameters, including free and total glycerol, acid value, sulfated ash, water content, and copper-strip corrosion, were not determined for the final FABE product. Consequently, no claim of complete certification or full SNI conformity is made in this study.

3.7. Analysis of FABE

The composition of the biodiesel product was analyzed using gas chromatography–mass spectrometry (GC–MS). The resulting chromatogram (Fig. 9) exhibits several distinct peaks within the retention time range of 5–35 min, indicating the presence of multiple fatty acid butyl ester (FABE) components.

The dominant chromatographic peak appeared at approximately 15 min and was assigned to butyl laurate based on the available mass-spectral library matching. Additional peaks were assigned to other putative FABE components, including butyl caprylate, butyl caprate, butyl myristate, butyl palmitate, butyl oleate, butyl linoleate, and butyl stearate. These assignments support the presence of butyl-ester species expected from coconut-oil fatty-acid composition; however, without authentic reference standards and a validated quantitative calibration, the GC–MS data are not used to establish absolute ester purity or standardized total ester content.

Relative GC–MS peak areas are reported only as a compositional profile of the detected compounds (Table 10). Because no internal standard or independently validated response-factor calibration was employed, the relative areas are not interpreted as quantitative mass fractions, ester purity, or standardized biodiesel conversion. A validated quantitative

Table 9.

Comparison of Selected FABE Fuel Properties with Corresponding SNI 7182:2015 Limits

Parameter	Unit	Product	SNI Standard (SNI 7182:2015)
Density (40 °C)	g/cm^3	0.850	0.85 – 0.89
Kinematic Viscosity (40 °C)	cSt	3.188	2.3 - 6
Flash Point	°C	103.4	min 100
Cetane Number	-	57.1	min 51

method, such as GC–FID with an appropriate internal standard and calibration procedure, would be required to determine standardized total ester content. Such analysis was not performed in the present study. The GC–MS profile is therefore qualitative to semi-quantitative, while the separately reported process yield is a gravimetric product-recovery metric.

4. Conclusion

This study demonstrates the feasibility of microwave-assisted transesterification for producing a coconut-oil-derived ester-rich product using butanol. FCCD optimization identified an operating region giving an approximately 98 % gravimetric product-recovery yield at a selected microwave output of 150 W and an optimum reaction time of 2.758 min. The corresponding nominal microwave energy associated with that output setting was approximately 0.0069 kWh per batch (≈25 kJ), excluding unmeasured magnetron conversion losses and auxiliary loads; it therefore should not be interpreted as total electrical energy consumption. The kinetic data were better described by an apparent pseudo-second-order model under the investigated conditions, and the calculated apparent activation energies are interpreted as lumped composition-dependent parameters rather than intrinsic molecular activation barriers. Density, kinematic viscosity, flash point, and cetane number were within the corresponding SNI 7182:2015 limits for those measured parameters only; full SNI compliance was not established. Likewise, GC–MS relative peak areas were used for compositional profiling and not as standardized quantitative ester purity. The principal limitations are the absence of verifiable feedstock FFA/acid-value/moisture data, independent replication of the single-factor screening experiments, direct total-energy measurements, microwave-compatible spatial temperature validation, quantitative total-ester analysis, and a complete butanol-recovery mass balance. Addressing these limitations will be important for rigorous validation, comparison with conventional heating, and future scale-up.

Acknowledgments

“This work was supported by the Government of Indonesia through the Center for Higher Education Funding and Assessment (PPAPT) Kemendiktisaintek, the Indonesian Endowment Fund for Education (LPDP), and the Indonesian Education Scholarship (BPI) under Grant No. 202414100794”.

Author Contributions : “I.P.: Investigation, Formal Analysis, Writing – Original Draft. S.S.: Methodology, Project Administration, Resources. M.M.: Conceptualization, Supervision, Validation,Writing – Review & Editing”.

Conflicts of Interest

“The authors declare no conflict of interest”.

References

Abdulkareem, H. A., Yassen, M. T., Ahmed, N. N., Ahmed, M. B., Gheni, S. A., Ali, M. M., Al-Sudani, F. T., & Tahah, A. K. (2026). Innovatively Engineered Biowaste-Derived CaO–Fe/Activated Carbon and Ce/Sepiolite Composite Catalysts for Microwave-Intensified Biodiesel Production from Waste Cooking oil. *Biochemical Engineering Journal*, 229, 110097. https://doi.org/10.1016/j.bej.2026.110097

Andreo-Martínez, P., García-Martínez, N., Durán-del-Amor, M. del M., & Quesada-Medina, J. (2018). Advances on Kinetics and Thermodynamics of Non-catalytic Supercritical Methanol Transesterification of Some Vegetable Oils to Biodiesel. *Energy Conversion and Management,* 173, 187–196. https://doi.org/10.1016/j.enconman.2018.07.069

Angassa, K., Tesfay, E., Weldmichael, T. G., & Kebede, S. (2023). Response Surface Methodology Process Optimization of Biodiesel Production from Castor Seed Oil. *Journal of Chemistry,* 2023, 6657732. https://doi.org/10.1155/2023/6657732

Anwar, M., Rasul, M. G., Ashwath, N., & Rahman, M. M. (2018). Optimisation of Second-Generation Biodiesel Production from Australian Native Stone Fruit Oil Using Response Surface Method. *Energies,* 11(10), 2566. https://doi.org/10.3390/en11102566

Aracil, J., El Boulifi, N., Bouaid, A., & Martinez, M. (2010). Process Optimization for Biodiesel Production from Corn Oil and Its Oxidative Stability. *International Journal of Chemical Engineering,* 2010, 518070. https://doi.org/10.1155/2010/518070

Asaad, S. M., Inayat, A., Jamil, F., Ghenai, C., & Shanableh, A. (2023). Optimization of Biodiesel Production from Waste Cooking Oil Using a Green Catalyst Prepared from Glass Waste and Animal Bones. *Energies,* 16(5), 2322. https://doi.org/10.3390/en16052322

Ashnani, M. H. M., Johari, A., Hashim, H., & Hasani, E. (2014). Life Cycle Assessment of Palm Oil Biodiesel Production in Malaysia. Applied Mechanics and Materials, 465–466, 1080–1086. https://doi.org/10.4028/www.scientific.net/amm.465-466.1080

Babaki, M., Yousefi, M., Habibi, Z., & Mohammadi, M. (2017). Process Optimization for Biodiesel Production from Waste Cooking Oil Using Multi-enzyme Systems through Response Surface Methodology. *Renewable Energy*, 105, 465–472. https://doi.org/10.1016/j.renene.2016.12.086

Badan Pusat Statistik. (2024). Luas Areal Tanaman Perkebunan Rakyat Menurut Jenis Tanaman (Ribu Hektar), 2021-2023. https://www.bps.go.id/id/statistics-table/2/MjU2OCMy/luas-areal-perkebunan-rakyat-menurut-jenis-tanaman.html

Badan Standardisasi Nasional. (2015). SNI 7182:2015 Syarat Mutu Biodiesel. www.bsn.go.id

Betiku, E., Okunsolawo, S. S., Ajala, S. O., & Odedele, O. S. (2015). Performance Evaluation of Artificial Neural Network Coupled with Generic Algorithm and Response Surface Methodology in Modeling and Optimization of Biodiesel Production Process Parameters from Shea Tree (Vitellaria paradoxa) Nut Butter. *Renewable Energy,* 76, 408–417. https://doi.org/10.1016/j.renene.2014.11.049

Cancela, A., Maceiras, R., Urrejola, S., & Sanchez, A. (2012). Microwave-Assisted Transesterification of Macroalgae. *Energies,* 5(4), 862–871. https://doi.org/10.3390/en5040862

Cercado, A. P. I., Ballesteros Jr, F. C., & Capareda, S. C. (2018). Biodiesel from Three Microalgae Transesterification Processes Using Different Homogenous Catalysts. *International Journal of Technology,* 9(4), 645–651. https://doi.org/10.14716/ijtech.v9i4.1145

Cevheroğlu Çira, S., Dağ, A., & Karakuş, A. (2016). Application of Response Surface Methodology and Central Composite Inscribed Design for Modeling and Optimization of Marble Surface Quality. Advances in Materials Science and Engineering, 2016, 2349476. https://doi.org/10.1155/2016/2349476

Chakraborty, R., & Bepari, S. (2012). Biodiesel Synthesis From Mustard Oil (Brassica Nigra) Using Calcium Oxide-Calcium Aluminate Catalyst Developed From Duck Eggshell. *International Journal Of Advanced Scientific Research And Technology*, 3(2), 242–256.

Chakraborty, R., Das, S., & Bhattacharjee, S. K. (2015). Optimization of Biodiesel Production from Indian Mustard Oil by Biological Tri-calcium Phosphate Catalyst Derived from Turkey Bone Ash. *Clean Technologies and Environmental Policy,* 17(2), 455–463. https://doi.org/10.1007/s10098-014-0802-z

Chakraborty, R., Das, S., Pradhan, P., & Mukhopadhyay, P. (2014). Prediction of Optimal Conditions in the Methanolysis of Mustard Oil for Biodiesel Production Using Cost-Effective Mg-Solid Catalysts. *Industrial & Engineering Chemistry Research,* 53(51), 19681–19689. https://doi.org/10.1021/ie501084z

Chen, H. Y., & Cui, Z. W. (2016). A Microwave-Sensitive Solid Acid Catalyst Prepared from Sweet Potato via a Simple Method. *Catalysts,* 6(12), 211. https://doi.org/10.3390/catal6120211

Chen, Q., & Qi, J. (2023). How Much Should We Trust R2 and Adjusted R2: Evidence from Regressions in Top Economics Journals and Monte Carlo Simulations. *Journal of Applied Economics*, 26(1), 2207326. https://doi.org/10.1080/15140326.2023.2207326

Chin, L. H., Hameed, B. H., & Ahmad, A. L. (2009). Process Optimization for Biodiesel Production from Waste Cooking Palm Oil (Elaeis guineensis) Using Response Surface Methodology. *Energy & Fuels,* 23(2), 1040–1044. https://doi.org/10.1021/ef8007954

Chua, C. B. H., Lee, H. M., & Low, J. S. C. (2010). Life Cycle Emissions and Energy Study of Biodiesel Derived From Waste Cooking Oil and Diesel in Singapore. *The International Journal of Life Cycle Assessment,* 15(4), 417–423. https://doi.org/10.1007/s11367-010-0166-5

Czyrski, A., & Jarzebski, H. (2020). Response Surface Methodology as a Useful Tool for Evaluation of the Recovery of the Fluoroquinolones from plasma-The Study on Applicability of Box-Behnken Design, Central Composite Design and Doehlert Design. *Processes,* 8(4), 473. https://doi.org/10.3390/PR8040473

Doori, W. H. A., Ali, O. M., Ahmed, A. H., & Koten, H. (2022). Comparative Study of Biodiesel Production from Different Waste Oil Sources for Optimum Operation Conditions and Better Engine Performance. *Journal of Thermal Engineering,* 8(4), 457–465. https://doi.org/10.18186/thermal.1135266

Ezzati, R., Ranjbar, S., & Soltanabadi, A. (2021). Kinetics Models of Transesterification Reaction for Biodiesel Production: A Theoretical Analysis. *Renewable Energy,* 168, 280–296. https://doi.org/10.1016/j.renene.2020.12.055

Fernández-Tirado, F., Parra-López, C., & Romero-Gámez, M. (2017). Evaluating the Environmental Sustainability of Energy Crops: A Life Cycle Assessment of Spanish Rapeseed and Argentinean Soybean Cultivation. Spanish *Journal of Agricultural Research*, 15(1), e0107. https://doi.org/10.5424/sjar/2017151-9287

Font de Mora, E., Torres, C., Valero, A., & Zambrana, D. (2013). Defossilisation Assessment of Biodiesel Life Cycle Production Using the ExROI Indicator. *International Journal of Thermodynamics,* 16(2), 81–86. https://doi.org/10.5541/ijot.452

Gaide, I., Makareviciene, V., Sendzikiene, E., & Gumbytė, M. (2023). Rapeseed Oil Transesterification Using 1-Butanol and Eggshell as a Catalyst. *Catalysts,* 13(2), 302. https://doi.org/10.3390/catal13020302

Garusti, G., Khuluq, A. D., Hartono, J., Riajaya, P. D., & Purwati, R. D. (2020). Karakteristik Biodiesel Kemiri Sunan dengan Katalis NaOH dan KOH. *Buletin Tanaman Tembakau, Serat & Minyak Industri*, 12(2), 78–85. https://doi.org/10.21082/btsm.v12n2.2020.78-85

Giraldi-Díaz, M. R., De Medina-Salas, L., Castillo-González, E., & De la Cruz-Benavides, M. (2018). Environmental Impact Associated With the Supply Chain and Production of Biodiesel From Jatropha Curcas L. Through Life Cycle Analysis. *Sustainability,* 10(5), 1451. https://doi.org/10.3390/su10051451

Gong, J., & You, F. (2015). Value-Added Chemicals From Microalgae: Greener, More Economical, or Both? *ACS Sustainable Chemistry & Engineering,* 3(1), 82–96. https://doi.org/10.1021/sc500683w

Gude, V. G., Patil, P., Martinez-Guerra, E., Deng, S., & Nirmalakhandan, N. (2013). Microwave Energy Potential for Biodiesel Production. *Sustainable Chemical Processes*, 1, 5. https://doi.org/10.1186/2043-7129-1-5

Hájek, M., Skopal, F., Vávra, A., & Kocík, J. (2017). Transesterification of rapeseed oil by butanol and separation of butyl ester. *Journal of Cleaner Production,* 155, 28–33. https://doi.org/10.1016/j.jclepro.2016.07.007

Handayani, P. A., Abdullah, A., & Hadiyanto, H. (2019). Response Surface Optimization of Biodiesel Production from Nyamplung (Calophyllum inophyllum) Oil Enhanced by Microwave and Ionic Liquid + NaOH Catalyst. *Periodica Polytechnica Chemical Engineering*, 63(3), 406–413. https://doi.org/10.3311/PPch.12965

Handayani, P. A., Abdullah, & Hadiyanto. (2018). Process Evaluation of Biodiesel Production from Nyamplung (Calophyllum inophyllum) Oil Enhanced by Ionic Liquid + NaOH Catalyst and Microwave Heating System. *Journal of Physical Science*, 29(Suppl. 2), 265–275. https://doi.org/10.21315/jps2018.29.s2.21

Harsono, S. S., Prochnow, A., Grundmann, P., Hansen, A., & Hallmann, C. (2012). Energy Balances and Greenhouse Gas Emissions of Palm Oil Biodiesel in Indonesia. *GCB Bioenergy,* 4(2), 213–228. https://doi.org/10.1111/j.1757-1707.2011.01118.x

Hazrat, M. A., Rasul, M. G., Khan, M. M. K., Ashwath, N., Silitonga, A. S., Fattah, I. M. R., & Mahlia, T. M. I. (2022). Kinetic Modelling of Esterification and Transesterification Processes for Biodiesel Production Utilising Waste-Based Resource. *Catalysts,* 12(11), 1472. https://doi.org/10.3390/catal12111472

Hou, J., Zhang, P., Yuan, X.-Z., & Yonghong, Z. (2011). Life Cycle Assessment of Biodiesel From Soybean, Jatropha and Microalgae in China Conditions. *Renewable and Sustainable Energy Reviews,* 15(9), 5081–5091. https://doi.org/10.1016/j.rser.2011.07.048

Hsiao, M. C., Liao, P. H., Lan, N. V., & Hou, S. S. (2021). Enhancement of Biodiesel Production from High-Acid-Value Waste Cooking Oil via a Microwave Reactor Using a Homogeneous Alkaline Catalyst. *Energies,* 14(2), 437. https://doi.org/10.3390/en14020437

International Coconut Community. (2024). Market Review of Dessicated Coconut June 2024. https://coconutcommunity.org/page-statistics/market-review/market-review-of-dessicated-coconut-june-2024

Iqbal, M. M. A., Bakar, W. A. W. A., Toemen, S., Razak, F. I. A., & Azelee, N. I. W. (2020). Optimization Study by Box-Behnken Design (BBD) and Mechanistic Insight of CO2 Methanation over Ru-Fe-Ce/γ-Al2O3 Catalyst by In-situ FTIR Technique. *Arabian Journal of Chemistry,* 13(2), 4170–4179. https://doi.org/10.1016/j.arabjc.2019.06.010

Kannan, R., Ramalingam, S., Sampath, S., Nedunchezhiyan, M., Dillikannan, D., & Jayabal, R. (2024). Optimization and Synthesis Process of Biodiesel Production from Coconut Oil using Central Composite Rotatable Design of Response Surface Methodology. *Proceedings of the Institution of Mechanical Engineers, Part E: Journal of Process Mechanical Engineering. Advance Online Publication.* https://doi.org/10.1177/09544089241230251

Kaushik, P., Kaur, G., & Hasan, I. (2024). Biodiesel Synthesis from Coconut Oil Using the Ash of Citrus limetta Peels as a Renewable Heterogeneous Catalyst. *Catalysts,* 14(8), 549. https://doi.org/10.3390/catal14080549

Khadivi, F., Samani, B. H., Rostami, S., Taki, K., Asghari, M., & Ghatrehsamani, S. (2025). Optimization and CFD-RSM Analysis of Single Orifice Reactor for Enhanced Biodiesel Production. *PLoS One*, 20(7), e0326747. https://doi.org/10.1371/journal.pone.0326747

Khan, H. M., Iqbal, T., Mujtaba, M. A., Soudagar, M. E. M., Veza, I., & Fattah, I. M. R. (2021). Microwave Assisted Biodiesel Production Using Heterogeneous Catalysts. *Energies,* 14(23), 8135. https://doi.org/10.3390/en14238135

Koech, A. K., Kumar, A., & Siagi, Z. O. (2020). In Situ Transesterification of Spirulina Microalgae to Produce Biodiesel Using Microwave Irradiation. *Journal of Energy,* 2020, 8816296. https://doi.org/10.1155/2020/8816296

Kumar, P., Ramprasad, M., & Sidharth. (2021). Optimized Biodiesel Preparation from Waste Cooking Oil as a Fuel for Unmodified Diesel Engines. *Journal of Engineering Research (Kuwait),* 2021, 1–18. https://doi.org/10.36909/jer.ICETET.14989

Kumar, R., & Sethy, A. K. (2015). Microwave Assisted Energy Efficient Biodiesel Production from Crude Pongamia pinnata (L.) Oil Using Homogeneous Catalyst. *Journal of Forest and Environmental Science,* 31(1), 1–6. https://doi.org/10.7747/JFES.2015.31.1.1

Kurczyński, D., Wcisło, G., Leśniak, A., Kozak, M., & Łagowski, P. (2022). Production and Testing of Butyl and Methyl Esters as New Generation Biodiesels from Fatty Wastes of the Leather Industry. *Energies*, 15(22), 8744. https://doi.org/10.3390/en15228744

Kurniati, S., Soeparman, S., Yuwono, S. S., Hakim, L., & Syam, S. (2019). A Novel Process for Production of Calophyllum Inophyllum Biodiesel with Electromagnetic Induction. *Energies,* 12(3), 383. https://doi.org/10.3390/en12030383

Maheswaran, R., & Uthranarayan, C. (2022). Effect of Photosynthetic Bacteria Based Feedstock and Temperature on Biodiesel Yield Using Microwave Assisted Transesterification With an Application of Box Behnken Supported Response Surface

Methodology. *Journal of the Chilean Chemical Society*, 67(3), 5636–5642. https://doi.org/10.4067/S0717-97072022000305636

Mahfud, M., Kalsum, U., & Aswie, V. (2020). Biodiesel Production through Catalytic Microwave In-Situ Transesterification of Microalgae (Chlorella sp.). International Journal of Renewable Energy Development, 9(1), 113–117. https://doi.org/10.14710/ijred.9.1.113-117

Mahfud, M., Rachmaditasari, R., Ansori, A., Suryanto, A., & Sardi, B. (2025). Optimization Using Box-Behnken Design of Biodiesel Synthesis: Microwave-Assisted Transesterification of Coconut Oil with Isopropyl Alcohol Using K2O/γ-Al2O3 Catalyst. *Biocatalysis and Agricultural Biotechnology,* 67, 103657. https://doi.org/10.1016/j.bcab.2025.103657

Mahfud, M., Suryanto, A., Qadariyah, L., Suprapto, S., & Kusuma, H. S. (2018). Production of Methyl Ester from Coconut Oil Using Microwave: Kinetic of Transesterification Reaction Using Heterogeneous CaO Catalyst. *Korean Chemical Engineering Research*, 56(2), 275–280. https://doi.org/10.9713/kcer.2018.56.2.275

Maliyekkal, M. N., & Shaija, A. (2021). Feasibility of Coconut Testa Oil and Coconut Waste Cooking Oil as Potential Biodiesel Feedstocks. Research Square. https://doi.org/10.21203/rs.3.rs-684031/v1

Milano, J., Tiong, S. K., Chia, S. R., Ong, M. Y., Sebayang, A. H., & Kalam, M. A. (2024). Production of Biodiesel from Non-edible Waste Palm Oil and Sterculia Foetida Using Microwave Irradiation. *IOP Conference Series: Earth and Environmental Science,* 1372(1), 012047. https://doi.org/10.1088/1755-1315/1372/1/012047

Mohammed, N. I., Kabbashi, N. A., Alam, M. Z., & Mirghani, M. E. S. (2021). Optimization of Jatropha Biodiesel Production by Response Surface Methodology. *Green and Sustainable Chemistry,* 11(1), 23–37. https://doi.org/10.4236/gsc.2021.111003

Mohanraj, J., Kannan, G. R., & Elango, M. (2022). Intensification of Biodiesel Production by Optimizing Process Parameters from Waste Cooking Oil through Response Surface Methodology. *IOP Conference Series: Earth and Environmental Science,* 1100(1), 012017. https://doi.org/10.1088/1755-1315/1100/1/012017

Montgomery, D. C. (2013). Design and Analysis of Experiments (8th ed.). John Wiley & Sons, Inc.

Musharavati, F., Sajid, K., Anwer, I., Nizami, A., Javed, M. H., Ahmad, A., & Naqvi, M. (2023). Advancing Biodiesel Production System From Mixed Vegetable Oil Waste: A Life Cycle Assessment of Environmental and Economic Outcomes. *Sustainability,* 15(24), 16550. https://doi.org/10.3390/su152416550

Nekkanti, V., Muniyappan, T., Karatgi, P., Hari, M. S., Marella, S., & Pillai, R. (2009). Spray-Drying Process Optimization for Manufacture of Drug – Cyclodextrin Complex Powder Using Design of Experiments. *Drug Development and Industrial Pharmacy,* 35(10), 1219–1229. https://doi.org/10.1080/03639040902882264

Niju, S., Vishnupriya, G., & Balajii, M. (2019). Process Optimization of Calophyllum inophyllum-waste Cooking Oil Mixture for Biodiesel Production Using Donax Deltoides Shells as Heterogeneous Catalyst. *Sustainable Environment Research*, 29, 18. https://doi.org/10.1186/s42834-019-0015-6

Nimcevic, D., Puntigam, R., Wörgetten, M., & Gapes, J. R. (2000). Preparation of Rapeseed Oil Esters of Lower Aliphatic Alcohols. JAOCS, *Journal of the American Oil Chemists' Society*, 77(3), 275–280. https://doi.org/10.1007/s11746-000-0045-1

Njoku, C. N., & Otisi, S. K. (2023). Application of Central Composite Design with Design Expert v13 in Process Optimization. Response Surface Methodology - Research Advances and Applications, 1–31. https://doi.org/10.5772/intechopen.109704

Nomanbhay, S., & Ong, M. Y. (2017). A Review of Microwave-Assisted Reactions for Biodiesel Production. *Bioengineering*, 4(2), 57. https://doi.org/10.3390/bioengineering4020057

Okpala, C. V., & Dibia, K. T. (2025). Optimized Biodiesel Production from Palm Kernel and Jatropha Curcas Oil Blend Using KOH-Supported Calcined Animal Bone Catalyst: A Response Surface Methodology and Genetic Algorithm-Bayesian Hybridization. *Cleaner Chemical Engineering*, 11, 100141. https://doi.org/10.1016/j.clce.2024.100141

Özgur, C., Tosun, E., & Özgur, T. (2017). Comparison of the Effects of Reaction Parameters on Cold Flow Properties of Biodiesel. MATTER: *International Journal of Science and Technology*, 3(3), 62–71. https://doi.org/10.20319/mijst.2017.33.6271

Qadariyah, L., Panjaitan, R., & Mahfud. (2021). Optimization Microwave Assisted Transesterification Insitu for Biodiesel Production from Chlorella sp. Using Response Surface Methodology. *IOP Conference Series: Earth and Environmental Science,* 743(1), 012090. https://doi.org/10.1088/1755-1315/743/1/012090

Rachmaditasari, R., Darojat, M. I., & Mahfud, M. (2024). Production of Biodiesel (Isopropyl Ester) from Coconut Oil by Microwave Assisted Transesterification: Parametric Study and Optimization. *International Journal of Renewable Energy Development*, 13(4), 662–672. https://doi.org/10.61435/ijred.2024.60174

Radojković, M., Zeković, Z., Jokić, S., & Vidović, S. (2012). Determination of Optimal Extraction Parameters of Mulberry Leaves Using Response Surface Methodology (RSM). *Romanian Biotechnological Letters,* 17(3), 7295–7308.

Refaat, A. A., El Sheltawy, S. T., & Sadek, K. U. (2008). Optimum Reaction Time, Performance and Exhaust Emissions of Biodiesel Produced by Microwave Irradiation. *International Journal of Environmental Science and Technology,* 5(3), 315–322. https://doi.org/10.1007/BF03326026

Renita, A. A., Sreedhar, N., & Magesh Peter, D. (2014). Optimization of Algal Methyl Esters Using RSM and Evaluation of Biodiesel Storage Characteristics. *Bioresources and Bioprocessing*, 1, 19. https://doi.org/10.1186/s40643-014-0019-3

Rhithuparna, D., Saha, B. B., Rokhum, S. L., & Halder, G. (2026). Advanced Non-catalytic Biodiesel Production Under Microwave Irradiation Using Waste Cooking Oil: Assessment of Scale-up Potential. *Renewable Energy*, 259, 125017. https://doi.org/10.1016/j.renene.2025.125017

Roushdy, M. H. (2022). Heterogeneous Biodiesel Catalyst from Steel Slag Resulting from an Electric Arc Furnace. *Processes,* 10(3), 465. https://doi.org/10.3390/pr10030465

Sánchez, M., Bergamin, F., Peña, E., Martínez, M., & Aracil, J. (2015). A Comparative Study of The Production of Esters from Jatropha Oil Using Different Short-Chain Alcohols: Optimization and Characterization. *Fuel,* 143, 183–188. https://doi.org/10.1016/j.fuel.2014.11.064

Seneviratne, K., & Jayathilaka, N. (2016). Coconut Oil: Chemistry and Nutrition (1st Ed.). Lakva Publishers.

Setiadji, S., Sundari, C. D. D., Munir, M., & Fitriyah, S. (2018). Synthesis of Solid Catalyst from Egg Shell Waste and Clay for Biodiesel Production. *Journal of Physics: Conference Series*, 1013(1), 012199. https://doi.org/10.1088/1742-6596/1013/1/012199

Sierra-Cantor, J. F., & Guerrero-Fajardo, C. A. (2017). Methods for Improving The Cold Flow Properties of Biodiesel with High Saturated Fatty Acids Content: A Review. *Renewable and Sustainable Energy Reviews,* 72, 774–790. https://doi.org/10.1016/j.rser.2017.01.077

Soliman, A., Ismail, A. R., Khater, M., Amr, S. A. A., El-Gendy, N. S., & Ezzat, A. A. (2024). Response Surface Optimization of a Single-Step Castor Oil–Based Biodiesel Production Process Using a Stator-Rotor Hydrodynamic Cavitation Reactor. *Environmental Science and Pollution Research*, 31(50), 60601–60618. https://doi.org/10.1007/s11356-024-35043-6

Souza, T. P. C., Silva, R. J. M. C. L., Melo, J. C., Tschoeke, I. C. P., Silva, J. P., Pacheco, J. G. A., & Silva, J. M. F. (2019). Kinetic Modeling of Cottonseed Oil Transesterification with Ethanol. *Reaction Kinetics, Mechanisms and Catalysis*, 128(2), 707–722. https://doi.org/10.1007/s11144-019-01661-2

Suryanto, A., Suprapto, S., & Mahfud, M. (2015). Production Biodiesel from Coconut Oil Using Microwave: Effect of Some Parameters on Transesterification Reaction by NaOH Catalyst. *Bulletin of Chemical Reaction Engineering and Catalysis*, 10(2), 162–168. https://doi.org/10.9767/bcrec.10.2.8080.162-168

Verdooren, L. R. (2017). Use of Doehlert Designs for Second-order Polynomial Models. *Mathematics and Statistics*, 5(2), 62–67. https://doi.org/10.13189/ms.2017.050202

Woo, C., Kook, S., Hawkes, E. R., Rogers, P. L., & Marquis, C. P. (2016). Dependency of Engine Combustion on Blending Ratio Variations of Lipase-Catalysed Coconut Oil Biodiesel and Petroleum Diesel. *Fuel*, 169, 146–157. https://doi.org/10.1016/j.fuel.2015.12.024

Yamin, J., Al-Hamamre, Z., & Sandouqa, A. (2024). Modelling and Optimisation of Biodiesel Production Using Waste Cooking Oil Using The Response Surface Methodology. *International Journal of Sustainable Energy,* 43(1), 2355654. https://doi.org/10.1080/14786451.2024.2355654

Yao, X., Wang, Z., Qian, M., Deng, Q., & Sun, P. (2024). Kinetic Aspects of Esterification and Transesterification in Microstructured Reactors. *Molecules,* 29(15), 3651. https://doi.org/10.3390/molecules29153651

Zabaruddin, N. H., Abdullah, L. C., Mohamed, N. H., & Choong, T. S. Y. (2020). Optimization Using Response Surface Methodology (RSM) for Biodiesel Synthesis Catalyzed by Radiation-Induced Kenaf Catalyst in Packed-Bed Reactor. *Processes,* 8(10), 1289. https://doi.org/10.3390/pr8101289

Zeng, D., Yang, L., & Fang, T. (2017). Process Optimization, Kinetic and Thermodynamic Studies on Biodiesel Production by Supercritical Methanol Transesterification with CH3ONa Catalyst. *Fuel,* 203, 739–748. https://doi.org/10.1016/j.fuel.2017.05.019

© 2026. The Author(s). This article is an open access article distributed under the terms and conditions of the Creative Commons Attribution-ShareAlike 4.0 (CC BY-SA) International License (http://creativecommons.org/licenses/by-sa/4.0/)